AN ENERGY STABLE FINITE ELEMENT SCHEME FOR THE THREE-COMPONENT CAHN-HILLIARD-TYPE MODEL FOR MACROMOLECULAR MICROSPHERE COMPOSITE HYDROGELS

MAOQIN YUAN, WENBIN CHEN, CHENG WANG, STEVEN M. WISE AND ZHENGRU ZHANG

ABSTRACT. In this article, we present and analyze a finite element numerical scheme for a three-component macromolecular microsphere composite (MMC) hydrogel model, which takes the form of a ternary Cahn-Hilliard-type equation with Flory-Huggins-deGennes energy potential. The numerical approach is based on a convex-concave decomposition of the energy functional in multi-phase space, in which the logarithmic and the nonlinear surface diffusion terms are treated implicitly, while the concave expansive linear terms are explicitly updated. A mass lumped finite element spatial approximation is applied, to ensure the positivity of the phase variables. In turn, a positivity-preserving property can be theoretically justified for the proposed fully discrete numerical scheme. In addition, unconditional energy stability is established as well, which comes from the convexity analysis. Several numerical simulations are carried out to verify the accuracy and positivity-preserving property of the proposed scheme.

AMS subject classifications: 35K25, 35K55, 60F10, 65M60

Keywords: MMC-TDGL equations, mass lumped FEM, convex-concave decomposition, energy stability, positivity preserving

1. INTRODUCTION

A hydrogel is a network of cross-linked hydrophilic polymers chains. They absorb water and can swell to many times their original size. Hydrogels, which can act as solids or liquids in various settings, are versatile materials that have led to extensive industrial and biomedical applications [20, 21, 33]. Macromolecular microsphere composite (MMC) hydrogel, which was originally synthesized by Huang et al. in 2007, possesses a unique well-defined network structure and very high mechanical strength. This is due to the highly specialized chemical grafting of the entangled polymer chains, in comparison with traditional hydrogels [31]. MMC hydrogels have been widely applied in both biomedical and industrial areas, such as in drug delivery [49], artificial tissues [12, 46], et cetera. The formation process of MMC hydrogel has been described in detail in [30, 31, 55].

Computational and experimental studies are needed to reveal the complicated properties of MMC hydrogels. Studies must include the investigation of the parameter space related to their production and processing, in order to engineer their individual effects. Furthermore, must be explored and refined to validate their predictions. For example, Zhai et al. [55] developed a reticular free energy for MMCs, under certain assumptions, most particularly, that the number of graft chains around a macromolecular microsphere (MMS) is proportional to the perimeter. Based on the time-dependent Ginzburg-Landau (TDGL) mesoscale simulation method, a two-component model, appropriately named the MMC-TDGL equation, was developed to understand the time evolution of MMC hydrogel structure in [55]. This continuum scale model was designed to simulate phase transitions in MMC hydrogels. Li et al. [34] added a stochastic term in the binary MMC-TDGL equation to consider how random physical fluctuations modify the dynamics. Recently, the reticular free energy was reconstructed in [32], and shown to be consistent with the network structures of the MMC hydrogels. Based on the Boltzmann entropy

theorem, the Flory-Huggins lattice theory and assuming TDGL dynamics, a three-component MMC-TDGL model can be constructed. The MMC and polymer chains are no longer considered as a whole in this model, making it more consistent with experiments.

It is widely known that phase-field models satisfy certain properties, such as energy decay, mass conservation, and positivity preservation. These properties represent important physical features and are also essential for mathematical analysis and consistent numerical simulation. During the past several decades, there have been many works devoted to designing various kinds of numerical methods to satisfy these properties, especially for Allen-Cahn and Cahn-Hilliard-type equations. See, for example, [10, 11, 48, 52, 54] and the references therein. Zhai et al. [55] constructed a spectral-type numerical method to approximate the solutions of the binary MMC-TDGL equations. Li et al. used a semi-implicit scheme for binary MMC-TDGL equation in [34], while there was no discussion of any stability condition. Subsequently, a convex splitting method was presented in [35], and energy stability was proven for the numerical solution of the phase variable. Liao et al. applied an adaptive time step strategy to improve computational efficiency in [36] and Dong et al. [18, 19] presented the theoretical analysis for the first and second-order energy stable schemes. A stabilized method was also used to solve the binary system by Xu et al. in [50], though a theoretical justification of the stabilizing parameters (for energy decay) has not been established. Other related works could be found in [25, 53], etc.

Although there have been many works on the multi-component Cahn-Hilliard flow [4, 5, 8, 54], addressing polynomial-type energy potentials, the numerical study of ternary MMC-TDGL equations is still in the preliminary stages. First, it has always been a key difficulty to design a numerical scheme satisfying the physical properties. Furthermore, it is highly challenging to prove the positivity-preserving property for the logarithmic terms, since the fourth-order partial differential equations fail to satisfy a maximum principle. In [11], a finite element scheme was proposed based on the backward Euler approximation for the Cahn-Hilliard equation with logarithmic free energy, and the positivity-preserving property of the numerical solution was proven under a constraint on the time step. In a more recent work [9], the authors presented a finite difference scheme based on the convex-concave decomposition of the free energy with logarithmic potential and established a theoretical justification of the positivity-preserving property, regardless of time step size. This improvement is based on the following fact: *the singular nature of the logarithmic term around the pure-phase values prevents the numerical solution from reaching these singular values, so that the numerical scheme is always well-defined as long as the numerical solution stays similarly bounded at the previous time step.* Moreover, similar ideas have been applied in [18, 19] to analyze the binary MMC-TDGL equation. Also see the related works of other gradient models with singular energy potential, such as the Poisson-Nernst-Planck system [38, 41], the reaction-diffusion system in the energetic variational formulation [37], liquid film droplet model [56], etc.

In this article, we aim to analyze the ternary MMC-TDGL system and obtain the theoretical justification of both the positivity-preserving property and the energy stability. To this end, the key ingredient is an application of the convex-concave decomposition of the physical energy, with respect to the multi-phase variables. In fact, the convex splitting method has been extensively applied to a variety of gradient flow models [2, 3, 6, 7, 15, 16, 23, 26–29, 39, 42, 44, 45, 47, 48, 51], for both first and second-order temporally accurate versions. Meanwhile, most of these existing works have focused on polynomial free energy potentials. The extension to singular Flory-Huggins-type energy potentials turns out to be highly challenging. In addition, the appearance of the highly nonlinear and singular deGennes gradient energy terms makes the whole system even more difficult. To overcome these subtle difficulties, we make use of a convex-concave decomposition of the physical energy in the ternary MMC-TDGL system, reported in a recent work [17].

In more details, the logarithmic terms and the highly nonlinear gradient energy terms are placed in the convex part, while the expansive terms are put in the concave part, based on careful convexity analyses. In turn, the convex splitting approach leads to a uniquely solvable, positivity-preserving and

energy stable numerical scheme. The finite difference approximation was reported in [17], and its direct application to the finite element method is not available, due to the difficulty to ensure the point-wise positivity of the numerical solution in the standard FEM method. In our work, a mixed FEM method is applied to the ternary MMC-TDGL system to facilitate the numerical implementation of the fourth order parabolic equations. It is well-known that the standard conforming FEM fails to satisfy the discrete maximum principle due to the non-diagonal mass matrix. As a result, a lumped mass FEM was chosen instead, so as to diagonalize the mass matrix. The diagonal elements are the row sums of the original mass matrix [43]. In comparison with the finite difference method, the FEM allows for flexible, adaptive meshes and is often easier to analyze.

This paper is organized as follows. In Section 2, we briefly review the mathematical model of three-component phase transitions in MMC hydrogels. In Section 3, we present the numerical scheme using the mass lumped finite element method. The detailed proof for the positivity-preserving property of the numerical solution is provided in Section 4, and the energy stability analysis is established in Section 5. In Section 6, the numerical simulations are presented to verify the theoretical results. Finally, some concluding remarks are given in Section 7.

2. Three-component MMC-TDGL system

Given an open bounded, connected domain $\Omega \subset \mathbb{R}^2$ with a Lipschitz smooth boundary $\partial\Omega$, we recall the derivation of the diffuse interface describing the phase transitions of MMC hydrogels. It is worth mentioning that the ternary system is made of water, macromolecular microsphere, and polymer chain. Usually, the composition of the mixture is described at each point by the concentration value of one of the constituents in the mixture. Thus we denote the concentration of the macromolecular microsphere in the ternary system by the order parameter ϕ_1, the polymer chain by ϕ_2 and the solvent molecules by ϕ_3. The value of the three order parameters are located between 0 and 1, where three phases vary rapidly but smoothly across the interface. And also, these three unknowns are linked through the hyperplain link relationship $\phi_1 + \phi_2 + \phi_3 = 1$. Due to the mass conservation constraint, we denote $\phi_3 = 1 - \phi_1 - \phi_2$ throughout the rest of this article, for simplicity of presentation.

The Flory-Huggins reticular free energy takes a form of $f(\phi_1, \phi_2)$. Moreover, the evolution of the system is driven by the minimization of a free energy under the constraint of mass conservation of each phase. The Ginzburg-Landau type energy functional $F(\phi_1, \phi_2)$ takes the following form

$$F(\phi_1, \phi_2) = \int_\Omega f(\phi_1, \phi_2) + K(\phi_1, \phi_2) d\mathbf{x}, \tag{2.1}$$

where $f(\phi_1, \phi_2)$ contains the mixing entropy $S(\phi_1, \phi_2)$ and the mixing enthalpy $H(\phi_1, \phi_2)$, i.e., $f(\phi_1, \phi_2) = S(\phi_1, \phi_2) + H(\phi_1, \phi_2)$. The expression of $S(\phi_1, \phi_2), H(\phi_1, \phi_2)$, as well as $K(\phi_1, \phi_2)$, can be written as follows

$$S(\phi_1, \phi_2) = \frac{\phi_1}{\gamma} \ln\left(\frac{\alpha\phi_1}{\gamma}\right) + \frac{\phi_2}{N} \ln\left(\frac{\beta\phi_2}{N}\right) + (1 - \phi_1 - \phi_2) \ln(1 - \phi_1 - \phi_2),$$

$$H(\phi_1, \phi_2) = \chi_{12}\phi_1\phi_2 + \chi_{13}\phi_1(1 - \phi_1 - \phi_2) + \chi_{23}\phi_2(1 - \phi_1 - \phi_2), \tag{2.2}$$

$$K(\phi_1, \phi_2) = \frac{a_1^2}{36\phi_1}|\nabla\phi_1|^2 + \frac{a_2^2}{36\phi_2}|\nabla\phi_2|^2 + \frac{a_3^2}{36(1 - \phi_1 - \phi_2)}|\nabla(1 - \phi_1 - \phi_2)|^2,$$

in which the parameter γ is the relative volume of one macromolecular microsphere, N is the degree of polymerization of the polymer chains. The parameters α and β are determined by the formulas $\alpha = \pi(\sqrt{\gamma/\pi} + N/2)^2, \beta = \alpha/\sqrt{\pi N}$, dependent on γ and N; see more detailed derivations of the model in [55]. In fact, the Flory-Huggins energy density takes a form of $\phi_i \ln \phi_i$ for each species concentration, combined with the interaction energy density $\phi_i\phi_j$ [24]. The constants χ_{12}, χ_{13}, and χ_{23} are the Flory-Huggins interaction parameters between macromolecular microspheres and polymer chain, macromolecular microspheres and solvent, and polymer chain and solvent, respectively. In addition, the deGennes diffusive coefficient, $\kappa(\phi_i) = \frac{a_i^2}{36\phi_i}$, depends on the corresponding phase variables. This

diffusion process was proposed by physicist P.G. deGennes [14] for the binary Cahn-Hilliard flow, in which the phase variables could be simplified as $\phi_1 = \phi$, $\phi_2 = 1 - \phi$, so that the combined diffusion coefficient and surface diffusion energy density becomes

$$\kappa(\phi) = \frac{a^2}{36\phi_1} + \frac{a^2}{36\phi_2} = \frac{a^2}{36\phi} + \frac{a^2}{36(1-\phi)} = \frac{a^2}{36\phi(1-\phi)}, \quad |\nabla\phi_1| = |\nabla\phi_2| = |\nabla\phi|,$$

$$K(\phi) = \frac{a^2}{36\phi_1}|\nabla\phi_1|^2 + \frac{a^2}{36\phi_2}|\nabla\phi_2|^2 = \kappa(\phi)|\nabla\phi|^2 = \frac{a^2}{36\phi(1-\phi)}|\nabla\phi|^2.$$

An extension to the ternary gradient flow is natural. Such a nonlinear diffusive coefficient has been an essential difficulty for the MMC-TDGL model; see the related analysis in [18, 19]. Here a_i is the statistical segment length of the ith component, $i = 1, 2, 3$. By a simple computation, the variational derivatives of the free energy function $F(\phi_1(\mathbf{x}, t), \phi_2(\mathbf{x}, t))$ with respect to ϕ_1 and ϕ_2 are found to be

$$\frac{\delta F(\phi_1, \phi_2)}{\delta \phi_1} = \frac{\partial S(\phi_1, \phi_2)}{\partial \phi_1} - \frac{a_1^2|\nabla\phi_1|^2}{36\phi_1^2} - \nabla \cdot \left(\frac{a_1^2\nabla\phi_1}{18\phi_1}\right) + \frac{a_3^2|\nabla(1-\phi_1-\phi_2)|^2}{36(1-\phi_1-\phi_2)^2} \tag{2.3}$$

$$+ \nabla \cdot \left(\frac{a_3^2\nabla(1-\phi_1-\phi_2)}{18(1-\phi_1-\phi_2)}\right) - \frac{\partial H(\phi_1, \phi_2)}{\partial \phi_1},$$

$$\frac{\delta F(\phi_1, \phi_2)}{\delta \phi_2} = \frac{\partial S(\phi_1, \phi_2)}{\partial \phi_2} - \frac{a_2^2|\nabla\phi_2|^2}{36\phi_2^2} - \nabla \cdot \left(\frac{a_2^2\nabla\phi_2}{18\phi_2}\right) + \frac{a_3^2|\nabla(1-\phi_1-\phi_2)|^2}{36(1-\phi_1-\phi_2)^2} \tag{2.4}$$

$$+ \nabla \cdot \left(\frac{a_3^2\nabla(1-\phi_1-\phi_2)}{18(1-\phi_1-\phi_2)}\right) - \frac{\partial H(\phi_1, \phi_2)}{\partial \phi_2},$$

where

$$\frac{\partial S}{\partial \phi_1} = \frac{1}{\gamma}\ln\left(\frac{\alpha\phi_1}{\gamma}\right) + \frac{1}{\gamma} - 1 - \ln(1 - \phi_1 - \phi_2), \quad \frac{\partial S}{\partial \phi_2} = \frac{1}{N}\ln\left(\frac{\beta\phi_2}{N}\right) + \frac{1}{N} - 1 - \ln(1 - \phi_1 - \phi_2),$$

$$\frac{\partial H}{\partial \phi_1} = -2\chi_{13}\phi_1 + (\chi_{12} - \chi_{13} - \chi_{23})\phi_2 + \chi_{13}, \quad \frac{\partial H}{\partial \phi_2} = -2\chi_{23}\phi_2 + (\chi_{12} - \chi_{13} - \chi_{23})\phi_1 + \chi_{23}.$$

To simulate the traditional hydrogels, the time-dependent Ginzburg-Landau (TDGL) mesoscopic model is widely used to describe the phase transitions of a multi-component polymer blend. Once this energy F is defined, we can formulate the time evolution of the three-component MMC hydrogels system for the conserved Cahn-Hilliard equations:

$$\frac{\partial \phi_1}{\partial t} = D_1 \Delta \frac{\delta F(\phi_1, \phi_2)}{\delta \phi_1}, \tag{2.5}$$

$$\frac{\partial \phi_2}{\partial t} = D_2 \Delta \frac{\delta F(\phi_1, \phi_2)}{\delta \phi_2}, \tag{2.6}$$

where $D_i = k_B\theta M_i$ are the diffusion coefficients, k_B is the Boltzmann constant, θ is the temperature, and $M_i > 0$ stand for the mobility of the ith component, $i = 1, 2$. For simplicity, we select $\Omega = (0, L)^2$, and consider L-periodic boundary condition for this model. However, the finite element method can be extended to a wider class of regions and Neumann boundary conditions could also be used.

The Cahn-Hilliard system has the important feature that the phase variables, ϕ_1 and ϕ_2, are mass-conservative. Integrating (2.5) and (2.6) over $\Omega = (0, L)^2$, we obtain

$$\frac{d}{dt}\int_\Omega \phi_1 d\mathbf{x} = \int_\Omega \frac{\partial \phi_1}{\partial t}d\mathbf{x} = D_1\int_{\partial\Omega}\nabla\frac{\delta F}{\delta\phi_1}\cdot\mathbf{n}ds,$$

$$\frac{d}{dt}\int_\Omega \phi_2 d\mathbf{x} = \int_\Omega \frac{\partial \phi_2}{\partial t}d\mathbf{x} = D_2\int_{\partial\Omega}\nabla\frac{\delta F}{\delta\phi_2}\cdot\mathbf{n}ds. \tag{2.7}$$

Notice that $\delta F/\delta\phi_1$ and $\delta F/\delta\phi_2$ in (2.3) and (2.4) are both L-periodic with respect to x and y, so that integration on the boundary vanishes, which implies

$$\int_\Omega \phi_1(\mathbf{x}, t)d\mathbf{x} = \int_\Omega \phi_1(\mathbf{x}, 0)d\mathbf{x}, \quad \int_\Omega \phi_2(\mathbf{x}, t)d\mathbf{x} = \int_\Omega \phi_2(\mathbf{x}, 0)d\mathbf{x}, \quad \forall t > 0. \tag{2.8}$$

As a consequence, $\phi_3 = 1 - \phi_1 - \phi_2$ also satisfies the mass-conversation property.

Meanwhile, the most distinguished difficulty for the Cahn-Hilliard equation with logarithmic Flory Huggins energy potential and deGennes diffusive coefficients is associated with the singularity as the value of ϕ approaches the limit value 0. In fact, for the binary Cahn-Hilliard flow, the positivity property, i.e., $0 < \phi_1, \phi_2$, has been established at the PDE analysis level in [1, 13, 22, 40]. As a further development, the phase separation has also been justified for the 1-D and 2-D equations at a theoretical level, i.e., a uniform distance between the phase variable and the singular limit values has been proved, and such a distance only depends on the surface diffusion coefficient and expansive parameter, as well as the initial data. For the ternary MMC TDGL model, a similar positivity estimate is expected to be valid for the exact PDE solution, i.e., $0 < \phi_i$, $(1 \le i \le 3)$, and a uniform separation property is also expected to be valid for 2-D flow; more technical details have to be involved for this model.

In terms of the energy stability, by multiplying (2.5) with $\delta F / \delta \phi_1$ and (2.6) with $\delta F / \delta \phi_2$, respectively, and integrating it over Ω, using Green's formula and the periodic boundary conditions, one obtains

$$
\begin{aligned}
\frac{dF}{dt} &= \int_\Omega \frac{\delta F}{\delta \phi_1} \frac{\partial \phi_1}{\partial t} d\mathbf{x} + \int_\Omega \frac{\delta F}{\delta \phi_2} \frac{\partial \phi_2}{\partial t} d\mathbf{x} \\
&= -D_1 \int_\Omega |\nabla \frac{\delta F}{\delta \phi_1}|^2 d\mathbf{x} - D_2 \int_\Omega |\nabla \frac{\delta F}{\delta \phi_2}|^2 d\mathbf{x} \le 0,
\end{aligned}
\tag{2.9}
$$

which indicates that the energy $F(\phi_1, \phi_2)$ is a decreasing function of time.

3. THE FULLY DISCRETE FINITE ELEMENT SCHEME

The standard notation for the norms is used, in their respective function spaces. In particular, we denote the standard norms for the Sobolev spaces $W^{m,p}(\Omega)$ by $\| \cdot \|_{m,p}$, and repleace $\| \cdot \|_{0,p}$ by $\| \cdot \|_p$, $\| \cdot \|_{0,2} = \| \cdot \|_2$ by $\| \cdot \|$, and $\| \cdot \|_{q,2}$ by $\| \cdot \|_{H^q}$. Let $C_{per}^\infty(\Omega)$ be the set of all restrictions onto Ω of all real-valued, L-periodic, $C^\infty(\Omega)$-functions on $\mathbb{R}^2$. For each integer $q \ge 0$, let $H_{per}^q(\Omega)$ be the closure of $C_{per}^\infty(\Omega)$ in the usual Sobolev norm $\| \cdot \|_q$, and $H_{per}^{-q}(\Omega)$ be the dual space of $H_{per}^q(\Omega)$. Note that $H_{per}^0(\Omega) = L^2(\Omega)$. In turn, by introducing $\mu_1 = \frac{\delta F}{\delta \phi_1} = \delta_{\phi_1} F$ and $\mu_2 = \frac{\delta F}{\delta \phi_2} = \delta_{\phi_2} F$, the mixed weak formulation of MMC-TDGL equations (2.5) becomes: find $\phi_1, \mu_1, \phi_2, \mu_2 \in L^2(0, T; H_{per}^1(\Omega))$, with $\partial_t \phi_1$, $\partial_t \phi_2 \in L^2(0, T; H_{per}^{-1}(\Omega))$, satisfying

$$
\begin{cases}
(\partial_t \phi_1, v_1) + (D_1 \nabla \mu_1, \nabla v_1) = 0, & \forall v_1 \in H_{per}^1(\Omega), \\
(\mu_1, w_1) = (\delta_{\phi_1} F(\phi_1, \phi_2), w_1), & \forall w_1 \in H_{per}^1(\Omega), \\
(\partial_t \phi_2, v_2) + (D_2 \nabla \mu_2, \nabla v_2) = 0, & \forall v_2 \in H_{per}^1(\Omega), \\
(\mu_2, w_2) = (\delta_{\phi_2} F(\phi_1, \phi_2), w_2), & \forall w_2 \in H_{per}^1(\Omega),
\end{cases}
\tag{3.1}
$$

for any $t \in [0, T]$, where $(\cdot, \cdot)$ represents the L^2 inner product or the duality pairing, as appropriate.

3.1. The finite element scheme. The following preliminary results are associated with the existence of the convex-concave decomposition of the energy functional F, i.e, $F(\phi_1, \phi_2)$ admits a (not necessarily unique) splitting into purely convex and concave energies, $F = F_c - F_e$, where $F_c = \int_\Omega S(\phi_1, \phi_2) + K(\phi_1, \phi_2) d\mathbf{x}$ and $F_e = -\int_\Omega H(\phi_1, \phi_2) d\mathbf{x}$ are convex with respect to the specific variables.

Proposition 3.1. *[17] Define the functions*

$$
\begin{aligned}
T_1(u, v) &:= \tfrac{v^2}{36u}, & u \in (0, \infty), & & v &\in \mathbb{R}; \\
T_2(u_1, u_2, v_1, v_2) &:= \tfrac{(v_1 + v_2)^2}{36(1 - u_1 - u_2)}, & u_1, u_2, v_1, v_2 &\in \mathbb{R}; \\
T_3(u, v, w) &:= \tfrac{w^2}{36(u+v)}, & u, v, w &\in \mathbb{R}; \\
T_4(u_1, u_2, u_3, v) &:= \tfrac{3v^2}{(u_1 + u_2 + u_3)} & u_1, u_2, u_3, v &\in \mathbb{R}.
\end{aligned}
$$

Then,

(1) $T_1(u, v)$ *is convex in* $(0, +\infty) \times \mathbb{R}$.

4

(2) $T_2(u_1, u_2, v_1, v_2)$ is convex in $\mathbb{R}^4$, provided $u_1 + u_2 < 1$.

(3) $T_3(u, v, w)$ is convex in $\mathbb{R}^3$, provided $u + v > 0$.

(4) $T_4(u_1, u_2, u_3, v)$ is convex in $\mathbb{R}^4$, provided $u_1 + u_2 + u_3 > 0$.

(5) $S(u_1, u_2)$ is convex in the Gibbs triangle $\mathcal{G}$, defined as

$$\mathcal{G} := \{(u_1, u_2) \mid u_1, u_2 > 0, u_1 + u_2 < 1\}.$$

(6) $H(u_1, u_2)$ is concave, provided that $4\chi_{13}\chi_{23} - (\chi_{12} - \chi_{13} - \chi_{23})^2 > 0$.

We consider a finite element method for solving (3.1). Let $\mathcal{T}_h$ be a shape-regular triangulation of Ω with mesh size h, denote h_e the diameter of each triangle $e \in \mathcal{T}_h$ and $\triangle_e$ the area of e. Noticing that the element is shape regular, we can assume that $\frac{h_e^2}{\triangle_e}$ is uniformly bounded by one constant $C_{\mathcal{T}}$: $\frac{h_e^2}{\triangle_e} \leq C_{\mathcal{T}}$. Based on the quasi-uniform triangulated mesh $\mathcal{T}_h$, the finite element space is defined as

$$S_h := \{v \in H^1_{per}(\Omega) \mid v \text{ is piecewise linear on each } e \in \mathcal{T}_h\} = \text{span}\{\chi_j \mid j = 1, \cdots, N_p\},$$

where χ_j is the common nodal basis function which is 1 at the node P_j and 0 at all other nodes. Define $\mathring{S}_h := S_h \cap L_0^2(\Omega)$, with $L_0^2(\Omega) = \{v \in L^2(\Omega) \mid (v, 1) = 0\}$, the function space with zero mean in $L^2(\Omega)$.

Definition 3.1. *The discrete energy $E : S_h \times S_h \to \mathbb{R}$ is defined as*

$$E(\phi_1, \phi_2) = \int_\Omega S(\phi_1, \phi_2) + H(\phi_1, \phi_2) + K(\phi_1, \phi_2) \, d\mathbf{x}.$$

Lemma 3.1. *Suppose that $\Omega = (0, L)^2$ and $\phi_1, \phi_2 \in S_h$ are periodic. Define the discrete energies as follows*

$$E_c = \int_\Omega S(\phi_1, \phi_2) + K(\phi_1, \phi_2) \, d\mathbf{x}, \quad E_e = -\int_\Omega H(\phi_1, \phi_2) \, d\mathbf{x}, \tag{3.2}$$

where $S(\cdot, \cdot), H(\cdot, \cdot)$ and $K(\cdot, \cdot)$ are defined by (2.2). Then, both $E_c(\phi_1, \phi_2)$ and $E_e(\phi_1, \phi_2)$ are convex.

Proof. Since $S_h \subset H^1_{per}(\Omega)$, the proof follows the analysis in Proposition 3.1, and the conclusions are obvious. $\square$

Then we introduce the fully-discrete scheme. Let M be a positive integer and $0 = t_0 < t_1 < \cdots < t_M = M\tau = T$ be a uniform partition of $[0, T]$, with $\tau = t_i - t_{i-1}$ and $i = 1, \cdots, M$. Due to the convex-concave decomposition $E = E_c - E_e$, the potentials could also be split into two parts, namely μ_1 and μ_2. By treating the convex term implicitly and the concave part explicitly, the first-order in time, mixed finite element scheme could be formulated as follows: for any $0 \leq n \leq M-1$, given $\phi_{1h}^n, \phi_{2h}^n \in S_h$, find $\phi_{1h}^{n+1}, \mu_{1h}^{n+1}, \phi_{2h}^{n+1}, \mu_{2h}^{n+1} \in S_h$ such that

$$\left(\frac{\phi_{1h}^{n+1} - \phi_{1h}^n}{\tau}, v_1\right) = -\left(D_1 \nabla \mu_{1h}^{n+1}, \nabla v_1\right), \qquad\qquad \forall v_1 \in \mathring{S}_h,$$

$$\left(\mu_{1h}^{n+1}, w_1\right) = \left(\delta_{\phi_1} E_c\left(\phi_{1h}^{n+1}, \phi_{2h}^{n+1}\right), w_1\right) + \left(\frac{\partial H}{\partial \phi_1}\left(\phi_{1h}^n, \phi_{2h}^n\right), w_1\right), \quad \forall w_1 \in \mathring{S}_h, \tag{3.3a}$$

$$\left(\frac{\phi_{2h}^{n+1} - \phi_{2h}^n}{\tau}, v_2\right) = -\left(D_2 \nabla \mu_{2h}^{n+1}, \nabla v_2\right), \qquad\qquad \forall v_2 \in \mathring{S}_h,$$

$$\left(\mu_{2h}^{n+1}, w_2\right) = \left(\delta_{\phi_2} E_c\left(\phi_{1h}^{n+1}, \phi_{2h}^{n+1}\right), w_2\right) + \left(\frac{\partial H}{\partial \phi_2}\left(\phi_{1h}^n, \phi_{2h}^n\right), w_2\right), \quad \forall w_2 \in \mathring{S}_h, \tag{3.3b}$$

where

$$\delta_{\phi_1} E_c\left(\phi_{1h}^{n+1}, \phi_{2h}^{n+1}\right) = \frac{\partial S}{\partial \phi_1}\left(\phi_{1h}^{n+1}, \phi_{2h}^{n+1}\right) + \delta_{\phi_1} K\left(\phi_{1h}^{n+1}, \phi_{2h}^{n+1}\right),$$

$$\delta_{\phi_2} E_c\left(\phi_{1h}^{n+1}, \phi_{2h}^{n+1}\right) = \frac{\partial S}{\partial \phi_2}\left(\phi_{1h}^{n+1}, \phi_{2h}^{n+1}\right) + \delta_{\phi_2} K\left(\phi_{1h}^{n+1}, \phi_{2h}^{n+1}\right), \tag{3.4}$$

and for $i = 1, 2$,

$$
\begin{aligned}
(\delta_{\phi_i} K(\phi_1, \phi_2), w) = & \left(-\frac{a_i^2 |\nabla \phi_i|^2}{36 \phi_i^2}, w \right) + \left(\frac{a_i^2 \nabla \phi_i}{18 \phi_i}, \nabla w \right) \\
& + \left(\frac{a_3^2 |\nabla (1 - \phi_1 - \phi_2)|^2}{36 (1 - \phi_1 - \phi_2)^2}, w \right) - \left(\frac{a_3^2 \nabla (1 - \phi_1 - \phi_2)}{18 (1 - \phi_1 - \phi_2)}, \nabla w \right).
\end{aligned}
$$

Definition 3.2. *The discrete Laplacian operator $\Delta_h : S_h \to \mathring{S}_h$ is defined as follows: for any $v_h \in S_h, \Delta_h v_h \in \mathring{S}_h$ denotes the unique solution to the problem*

$$
(\Delta_h v_h, \chi) = - (\nabla v_h, \nabla \chi), \quad \forall \chi \in S_h.
$$

It is straightforward to show that by restricting the domain, $\Delta_h : \mathring{S}_h \to \mathring{S}_h$ is invertible, and for any $v_h \in \mathring{S}_h$, and we have

$$
\left(\nabla (-\Delta_h)^{-1} v_h, \nabla \chi \right) = (v_h, \chi), \quad \forall \chi \in S_h.
$$

Definition 3.3. *The discrete H^{-1} norm $\| \cdot \|_{-1,h}$, is defined as follows:*

$$
\|v_h\|_{-1,h} := \sqrt{(v_h, (-\Delta_h)^{-1} v_h)}, \quad \forall v_h \in \mathring{S}_h. \tag{3.5}
$$

Lemma 3.2. *Suppose that $\Omega = (0, L)^2$ and $\phi_1, \phi_2, \psi_1, \psi_2 \in S_h$ are periodic. Consider the convex-concave decomposition of the energy $E(\phi_1, \phi_2)$ into $E = E_c - E_e$. Then we have*

$$
\begin{aligned}
E(\phi_1, \phi_2) - E(\psi_1, \psi_2) \leqslant & (\delta_{\phi_1} E_c(\phi_1, \phi_2) - \delta_{\phi_1} E_e(\psi_1, \psi_2), \phi_1 - \psi_1) \\
& + (\delta_{\phi_2} E_c(\phi_1, \phi_2) - \delta_{\phi_2} E_e(\psi_1, \psi_2), \phi_2 - \psi_2),
\end{aligned} \tag{3.6}
$$

where δ_{ϕ_1} and δ_{ϕ_2} denote the variational derivatives.

Proof. Define

$$
\begin{aligned}
e_c(\mathbf{u}, \mathbf{p}) &= S(u, p) + T_1(u, u_x) + T_1(u, u_y) + T_1(p, p_x) + T_1(p, p_y) + T_2(u, p, u_x, p_x) + T_2(u, p, u_y, p_y), \\
e_e(\mathbf{u}, \mathbf{p}) &= -H(u, p),
\end{aligned}
$$

where $\mathbf{u} = (u, u_x, u_y), \mathbf{p} = (p, p_x, p_y)$. The following identities are obvious

$$
E_c = \int_\Omega e_c(\mathbf{u}, \mathbf{p}) d\mathbf{x}, \quad E_e = \int_\Omega e_e(\mathbf{u}, \mathbf{p}) d\mathbf{x}.
$$

We know that both $e_c(\mathbf{u}, \mathbf{p})$ and $e_e(\mathbf{u}, \mathbf{p})$ are convex on $((0, 1) \times \mathbb{R} \times \mathbb{R})^2$. Then we have

$$
e_c(\mathbf{v}, \mathbf{p}) - e_c(\mathbf{u}, \mathbf{p}) \geq \nabla_{\mathbf{u}} e_c(\mathbf{u}, \mathbf{p}) \cdot (\mathbf{v} - \mathbf{u}).
$$

Next, setting $\mathbf{u} = (\phi_1, \phi_{1x}, \phi_{1y}), \mathbf{v} = (\psi_1, \psi_{1x}, \psi_{1y}), \mathbf{p} = (\phi_2, \phi_{2x}, \phi_{2y})$, one obtains

$$
\begin{aligned}
E_c(\psi_1, \phi_2) - E_c(\phi_1, \phi_2) \geq & \int_\Omega \partial_{\phi_1} e_c(\mathbf{u}, \mathbf{p})(\psi_1 - \phi_1) + \partial_{\phi_{1x}} e_c(\mathbf{u}, \mathbf{p})(\psi_{1x} - \phi_{1x}) \\
& + \partial_{\phi_{1y}} e_c(\mathbf{u}, \mathbf{p})(\psi_{1y} - \phi_{1y}) d\mathbf{x} \\
= & (\delta_{\phi_1} E_c(\phi_1, \phi_2), \psi_1 - \phi_1).
\end{aligned}
$$

Similarly, the following inequality could be derived for E_e:

$$
E_e(\phi_1, \phi_2) - E_e(\psi_1, \phi_2) \geq (\delta_{\phi_1} E_e(\psi_1, \phi_2), \phi_1 - \psi_1).
$$

Then the following estimate holds

$$
\begin{aligned}
E(\psi_1, \phi_2) - E(\phi_1, \phi_2) &= E_c(\psi_1, \phi_2) - E_e(\psi_1, \phi_2) - (E_c(\phi_1, \phi_2) - E_e(\phi_1, \phi_2)) \\
&= E_c(\psi_1, \phi_2) - E_c(\phi_1, \phi_2) - (E_e(\psi_1, \phi_2) - E_e(\phi_1, \phi_2)) \\
&\geq (\delta_{\phi_1} E_c(\phi_1, \phi_2), \psi_1 - \phi_1) + (\delta_{\phi_1} E_e(\psi_1, \phi_2), \phi_1 - \psi_1) \\
&\geq (\delta_{\phi_1} E_c(\phi_1, \phi_2) - \delta_{\phi_1} E_e(\psi_1, \phi_2), \psi_1 - \phi_1),
\end{aligned}
$$

6

and we get

$$E(\phi_1, \phi_2) - E(\psi_1, \phi_2) \le (\delta_{\phi_1} E_c(\phi_1, \phi_2) - \delta_{\phi_1} E_e(\psi_1, \phi_2), \phi_1 - \psi_1).$$

A similar inequality could be derived in the same fashion:

$$E(\psi_1, \phi_2) - E(\psi_1, \psi_2) \le (\delta_{\phi_2} E_c(\psi_1, \phi_2) - \delta_{\phi_2} E_e(\psi_1, \psi_2), \phi_2 - \psi_2).$$

To sum up, the proof is completed. □

3.2. **The mass lumped finite element method.** The standard mixed FEM (3.3) leads to a theoretical difficulty for justifying the positivity-preserving property. To overcome this subtle difficulty, we apply a mass lumped FEM instead, which is a modification of standard conforming FEM for solving parabolic equations. It simplifies the computation for the inverse of a mass matrix and overcomes the shortcoming of the standard FEM that can not preserve the maximum principle for homogeneous parabolic equations. In this subsection, we extend the lumped mass FEM to solve MMC-TDGL equations.

Let $P_{e,k}(k = i, j, m)$ be the vertices of triangle e, and $\triangle_e$ be the area of triangle e. The generation of the lumped mass matrix can be regarded as introducing the following quadrature formula:

$$Q_h(f) = \sum_{e \in \mathcal{T}_h} Q_e(f), \tag{3.7}$$

where

$$Q_e(f) = \frac{\triangle_e}{3} \sum_{k=i,j,m} f(P_{e,k}) \approx \int_e f d\mathbf{x}.$$

By the above quadrature formula, it is easy to derive $Q_h(\chi_j, \chi_k) = 0$ for $k \ne j$, so that

$$\sum_{k=1}^{N_p} (\chi_j, \chi_k) = Q_h(\chi_j^2). \tag{3.8}$$

Notice that $\chi_j \chi_k$ is a second-degree polynomial, thus it holds that $(\chi_j, \chi_k)_e = \frac{1}{12}\triangle_e$ for $k \ne j$, and $(\chi_j, \chi_j)_e = \frac{1}{6}\triangle_e$. Then we get

$$\sum_{k=1}^{N_p} (\chi_j, \chi_k) = \frac{1}{3} \operatorname{area}(D_j), \tag{3.9}$$

where D_j is the union of triangles with a vertex P_j. It is obvious that

$$Q_h(\chi_j^2) = \sum_{e \in \mathcal{T}_h} Q_e(\chi_j^2) = \frac{1}{3} \operatorname{area}(D_j). \tag{3.10}$$

We may then define an approximation of the inner product in S_h by

$$(\psi, \eta)_Q = Q_h(\psi\eta), \tag{3.11}$$

thus $\|\eta\|_Q = \sqrt{(\eta, \eta)_Q}$ can be denoted as a norm for any $\eta \in S_h$ and is equivalent to the standard $\|\cdot\|_{L^2}$ norm by considering each triangle separately.

To facilitate the analysis below, we have to modify the definition of the discrete Laplacian operator and the discrete H^{-1} norm. In fact, the primary difference is in the integral definition.

Definition 3.4. *The discrete Laplacian operator $\Delta_h : S_h \to \mathring{S}_h$ is defined as follows: for any $v_h \in S_h, \Delta_h v_h \in \mathring{S}_h$ denote the unique solution to the problem*

$$(\Delta_h v_h, \chi)_Q = -(\nabla v_h, \nabla \chi), \quad \forall \chi \in S_h.$$

It is straightforward to show that by restricting the domain, $\Delta_h : \mathring{S}_h \to \mathring{S}_h$ is invertible, and for any $v_h \in \mathring{S}_h$, and we have

$$\left(\nabla(-\Delta_h)^{-1} v_h, \nabla \chi\right) = (v_h, \chi)_Q, \quad \forall \chi \in S_h.$$

Definition 3.5. *The discrete H^{-1} norm $\| \cdot \|_{-1,Q}$, is defined as follows:*

$$\|v_h\|_{-1,Q} := \sqrt{(v_h, (-\Delta_h)^{-1} v_h)_Q}, \quad \forall v_h \in \mathring{S}_h. \tag{3.12}$$

Definition 3.6. *Define the discrete energy $\hat{E} : S_h \times S_h \to \mathbb{R}$ as follows*

$$\hat{E}(\phi_1, \phi_2) = (S(\phi_1, \phi_2))_Q + (H(\phi_1, \phi_2))_Q + (\tilde{K}(\phi_1, \phi_2), 1) \tag{3.13}$$

where

$$\tilde{K}(\phi_1, \phi_2) := \sum_{\ell=1}^{3} \frac{a_\ell^2}{36} \frac{|\nabla \phi_\ell|^2}{A(\phi_\ell)}, \tag{3.14}$$

and the operator A represents element average operator, that is,

$$A(\phi)|_e = \frac{1}{\triangle_e} \int_e \phi d\mathbf{x} = \frac{1}{3}(\phi_\alpha + \phi_\beta + \phi_\gamma).$$

In the last equation, ϕ_α, ϕ_β, and ϕ_γ, are the values of ϕ at the three vertices of the element e.

Lemma 3.3. *(Existence of a convex-concave decomposition). Suppose $(\phi_1, \phi_2) \in S_h$. The functions*

$$\hat{E}_c = (S(\phi_1, \phi_2))_Q + (\tilde{K}(\phi_1, \phi_2), 1), \tag{3.15}$$

$$\hat{E}_e = (-H(\phi_1, \phi_2))_Q, \tag{3.16}$$

are convex. Therefore, $\hat{E}(\phi_1, \phi_2) = \hat{E}_c(\phi_1, \phi_2) - \hat{E}_e(\phi_1, \phi_2)$ is a convex-concave decomposition of the discrete energy.

Proof. The convex-concave decomposition is easily obtained by applying Proposition 3.1. $\qquad\square$

In turn, the lumped mass form of (3.3) becomes: for given $\phi_{1h}^n, \phi_{2h}^n \in S_h$, find $\phi_{1h}^{n+1}, \mu_{1h}^{n+1}, \phi_{2h}^{n+1}, \mu_{2h}^{n+1} \in S_h$ such that

$$\left(\frac{\phi_{1h}^{n+1} - \phi_{1h}^n}{\tau}, v_1 \right)_Q = -\left(D_1 \nabla \mu_{1h}^{n+1}, \nabla v_1 \right), \tag{3.17a}$$

$$\left(\mu_{1h}{}^{n+1}, w_1 \right)_Q = \left(\delta_{\phi_1} S \left(\phi_{1h}^{n+1}, \phi_{2h}^{n+1} \right), w_1 \right)_Q + \left(\delta_{\phi_1} \tilde{K} \left(\phi_{1h}^{n+1}, \phi_{2h}^{n+1} \right), w_1 \right) \tag{3.17b}$$
$$+ \left(\delta_{\phi_1} H \left(\phi_{1h}^n, \phi_{2h}^n \right), w_1 \right)_Q,$$

$$\left(\frac{\phi_{2h}^{n+1} - \phi_{2h}^n}{\tau}, v_2 \right)_Q = -\left(D_2 \nabla \mu_{2h}^{n+1}, \nabla v_2 \right), \tag{3.17c}$$

$$\left(\mu_{2h}{}^{n+1}, w_2 \right)_Q = \left(\delta_{\phi_2} S \left(\phi_{1h}^{n+1}, \phi_{2h}^{n+1} \right), w_2 \right)_Q + \left(\delta_{\phi_2} \tilde{K} \left(\phi_{1h}^{n+1}, \phi_{2h}^{n+1} \right), w_2 \right) \tag{3.17d}$$
$$+ \left(\delta_{\phi_2} H \left(\phi_{1h}^n, \phi_{2h}^n \right), w_2 \right)_Q,$$

where for $i = 1, 2$,

$$(\delta_{\phi_i} \tilde{K} (\phi_1, \phi_2), w) = \left(-\frac{a_i^2 |\nabla \phi_i|^2}{36(A(\phi_i))^2}, w \right) + \left(\frac{a_i^2 \nabla \phi_i}{18 A(\phi_i)}, \nabla w \right)$$

$$+ \left(\frac{a_3^2 |\nabla (1 - \phi_1 - \phi_2)|^2}{36 (1 - A(\phi_1) - A(\phi_2))^2}, w \right) - \left(\frac{a_3^2 \nabla (1 - \phi_1 - \phi_2)}{18 (1 - A(\phi_1) - A(\phi_2))}, \nabla w \right).$$

In addition, the following lemma is needed for the later analysis.

Lemma 3.4. *Suppose that $\Omega = (0, L)^2$ and $\phi_1, \phi_2, \varphi_1, \varphi_2 : \Omega \to \mathbb{R}$ are periodic and sufficiently regular. Consider the convex-concave decomposition of the energy $\hat{E}(\phi_1, \phi_2)$ into $\hat{E} = \hat{E}_c - \hat{E}_e$, given by (3.15)-(3.16), then we have*

$$\hat{E}(\phi_1, \phi_2) - \hat{E}(\varphi_1, \varphi_2) \leq \left(\frac{\partial}{\partial \phi_1} S(\phi_1, \phi_2) + \frac{\partial}{\partial \phi_1} H(\phi_1, \phi_2), \varphi_1 - \phi_1 \right)_Q + (\delta_{\phi_1} \tilde{K}(\phi_1, \phi_2), \varphi_1 - \phi_1)$$

$$+\left(\frac{\partial}{\partial\phi_2}S(\phi_1,\phi_2)+\frac{\partial}{\partial\phi_2}H(\phi_1,\phi_2),\varphi_2-\phi_2\right)_Q+(\delta_{\phi_2}\tilde{K}(\phi_1,\phi_2),\varphi_2-\phi_2).$$

Proof. Fix $(\phi_1,\phi_2)\in S_h\times S_h$ and $(\psi_1,\psi_2)\in S_h\times S_h$. For any $0<\lambda<1$, we can define the continuous and differentiable function $J_c(\lambda):=\hat{E}_c(\phi_1+\lambda\psi_1,\phi_2+\lambda\psi_2)$. Since $\hat{E}_c(\phi_1,\phi_2)$ is convex, $J_c(\lambda)$ is convex. We have $J_c(\lambda)-J_c(0)\geq J_c'(0)\lambda$. This implies that

$$\hat{E}_c(\phi_1+\lambda\psi_1,\phi_2+\lambda\psi_2)-\hat{E}_c(\phi_1,\phi_2)\geq\left(\frac{\partial}{\partial\phi_1}S(\phi_1,\phi_2),\lambda\psi_1\right)_Q+\left(\frac{\partial}{\partial\phi_2}S(\phi_1,\phi_2),\lambda\psi_2\right)_Q \tag{3.18}$$
$$-\left(\frac{a_1^2|\nabla\phi_1|^2}{36(A(\phi_1))^2},\lambda\psi_1\right)+\left(\frac{a_1^2\nabla\phi_1}{18A(\phi_1)},\lambda\nabla\psi_1\right)$$
$$+\left(\frac{a_3^2|\nabla(1-\phi_1-\phi_2)|^2}{36(A(1-\phi_1-\phi_2))^2},\lambda\psi_1\right)-\left(\frac{a_3^2\nabla(1-\phi_1-\phi_2)}{18A(1-\phi_1-\phi_2)},\lambda\nabla\psi_1\right)$$
$$-\left(\frac{a_2^2|\nabla\phi_2|^2}{36(A(\phi_2))^2},\lambda\psi_2\right)+\left(\frac{a_2^2\nabla\phi_2}{18A(\phi_2)},\lambda\nabla\psi_2\right)$$
$$+\left(\frac{a_3^2|\nabla(1-\phi_1-\phi_2)|^2}{36(A(1-\phi_1-\phi_2))^2},\lambda\psi_2\right)-\left(\frac{a_3^2\nabla(1-\phi_1-\phi_2)}{18A(1-\phi_1-\phi_2)},\lambda\nabla\psi_2\right).$$

We may assume that $(\varphi_1,\varphi_2):=(\phi_1,\phi_2)+\lambda(\psi_1,\psi_2)\in S_h\times S_h$, since λ is small in magnitude. Then we have

$$\hat{E}_c(\varphi_1,\varphi_2)-\hat{E}_c(\phi_1,\phi_2)\geq\left(\frac{\partial}{\partial\phi_1}S(\phi_1,\phi_2),\varphi_1-\phi_1\right)_Q+\left(\frac{\partial}{\partial\phi_2}S(\phi_1,\phi_2),\varphi_2-\phi_2\right)_Q \tag{3.19}$$
$$-\left(\frac{a_1^2|\nabla\phi_1|^2}{36(A(\phi_1))^2},\varphi_1-\phi_1\right)+\left(\frac{a_1^2\nabla\phi_1}{18A(\phi_1)},\nabla(\varphi_1-\phi_1)\right)$$
$$+\left(\frac{a_3^2|\nabla(1-\phi_1-\phi_2)|^2}{36(A(1-\phi_1-\phi_2))^2},\varphi_1-\phi_1\right)-\left(\frac{a_3^2\nabla(1-\phi_1-\phi_2)}{18A(1-\phi_1-\phi_2)},\nabla(\varphi_1-\phi_1)\right)$$
$$-\left(\frac{a_2^2|\nabla\phi_2|^2}{36(A(\phi_2))^2},\varphi_2-\phi_2\right)+\left(\frac{a_2^2\nabla\phi_2}{18A(\phi_2)},\nabla(\varphi_2-\phi_2)\right)$$
$$+\left(\frac{a_3^2|\nabla(1-\phi_1-\phi_2)|^2}{36(A(1-\phi_1-\phi_2))^2},\varphi_2-\phi_2\right)-\left(\frac{a_3^2\nabla(1-\phi_1-\phi_2)}{18A(1-\phi_1-\phi_2)},\nabla(\varphi_2-\phi_2)\right).$$

For $\hat{E}_e$, a similar inequality is available:

$$\hat{E}_e(\varphi_1,\varphi_2)-\hat{E}_e(\phi_1,\phi_2)\geq\left(-\frac{\partial}{\partial\phi_1}H(\phi_1,\phi_2),\varphi_1-\phi_1\right)_Q+\left(-\frac{\partial}{\partial\phi_2}H(\phi_1,\phi_2),\varphi_2-\phi_2\right)_Q. \tag{3.20}$$

Combining the inequalities, we have

$$\hat{E}(\phi_1,\phi_2)-\hat{E}(\varphi_1,\varphi_2)=(\hat{E}_c(\phi_1,\phi_2)-\hat{E}_c(\varphi_1,\varphi_2))-(\hat{E}_e(\phi_1,\phi_2)-\hat{E}_e(\varphi_1,\varphi_2)) \tag{3.21}$$
$$\leq\left(\frac{\partial}{\partial\phi_1}S(\phi_1,\phi_2),\phi_1-\varphi_1\right)_Q+(\delta_{\phi_1}\tilde{K}(\phi_1,\phi_2),\phi_1-\varphi_1)$$
$$+\left(\frac{\partial}{\partial\phi_2}S(\phi_1,\phi_2),\phi_2-\varphi_2\right)_Q+(\delta_{\phi_2}\tilde{K}(\phi_1,\phi_2),\phi_2-\varphi_2)$$
$$-\left(-\frac{\partial}{\partial\phi_1}H(\phi_1,\phi_2),\phi_1-\varphi_1\right)_Q-\left(-\frac{\partial}{\partial\phi_2}H(\phi_1,\phi_2),\phi_2-\varphi_2\right)_Q.$$

Consequently, the proof is completed. $\qquad\square$

Remark 3.1. *The periodic boundary condition is considered in this article, for simplicity of presentation, since all the boundary integral terms will cancel, so that the integration by parts is always valid. As a result, for all the nonlinear and singular terms, the boundary terms will cause any scientific difficulty in the mathematical analysis. Meanwhile, the analysis in this work could be extended to other type of physically relevant boundary condition, such a homogeneous Neumann one. In fact, a natural boundary*

condition (corresponding to the Neumann boundary one) is more straightforward in the finite element set-up, and this extension analysis will be considered in the future works.

4. The unique solvability and positivity-preserving property

The mass lumped method, improving the original mass matrix, provides us with an efficient way to derive the theoretical proof of preserving positivity property for the MMC-TDGL equations.

Lemma 4.1. [9] Suppose that $\xi, \bar{\xi} \in S_h$, with $(\xi - \bar{\xi}, 1) = 0$, that is, $\xi - \bar{\xi} \in \mathring{S}_h$, and assume that $\|\xi\|_\infty < 1, \|\bar{\xi}\|_\infty \leq M$. Then, we have the following estimate:

$$\left\| -\Delta_h^{-1} \left(\xi - \bar{\xi} \right) \right\|_\infty \leq C_1, \tag{4.1}$$

where $C_1 > 0$ depends only upon M and Ω. In particular, C_1 is independent of the mesh spacing h .

Lemma 4.2. Let $\phi, \psi \in S_h$ and $A(\psi) > 0$, then

$$\left(-\frac{|\nabla \phi|^2}{36(A(\phi))^2}, \psi \right) + \left(\frac{\nabla \phi}{18A(\phi)}, \nabla \psi \right) \leq \frac{1}{36} \left(\frac{\nabla \psi}{A(\psi)}, \nabla \psi \right), \tag{4.2}$$

$$\left(\frac{|\nabla \phi|^2}{36(A(\phi))^2}, \psi \right) - \left(\frac{\nabla \phi}{18A(\phi)}, \nabla \psi \right) \leq \left(\frac{|\nabla \phi|^2}{18(A(\phi))^2}, A(\psi) \right) + \frac{1}{36} \left(\frac{\nabla \psi}{A(\psi)}, \nabla \psi \right). \tag{4.3}$$

Proof. By Cauchy-Schwarz inequality, on every element $e \in \mathcal{T}_h$, one gets

$$\left| \left(\frac{\nabla \phi}{18A(\phi)}, \nabla \psi \right)_e \right| \leq \left(\frac{|\nabla \phi|^2}{36(A(\phi))^2}, A(\psi) \right)_e^{\frac{1}{2}} \left(\frac{\nabla \psi}{9A(\psi)}, \nabla \psi \right)_e^{\frac{1}{2}}$$

$$\leq \left(\frac{|\nabla \phi|^2}{36(A(\phi))^2}, A(\psi) \right)_e + \left(\frac{\nabla \psi}{36A(\psi)}, \nabla \psi \right)_e. \tag{4.4}$$

Summing over all e,

$$\left| \left(\frac{\nabla \phi}{18A(\phi)}, \nabla \psi \right) \right| \leq \left(\frac{|\nabla \phi|^2}{36(A(\phi))^2}, A(\psi) \right) + \left(\frac{\nabla \psi}{36A(\psi)}, \nabla \psi \right). \tag{4.5}$$

Moreover, note that for $\phi, \psi \in S_h$,

$$\left(-\frac{|\nabla \phi|^2}{36(A(\phi))^2}, \psi \right) = \left(-\frac{|\nabla \phi|^2}{36(A(\phi))^2}, A(\psi) \right),$$

then the lemma can be proved by combining this relationship with (4.5). □

Remark 4.1. If $A(\psi) \geq 0$, then Lemma 4.2 will be modified by

$$\left(-\frac{|\nabla \phi|^2}{36(A(\phi))^2}, \psi \right) + \left(\frac{\nabla \phi}{18A(\phi)}, \nabla \psi \right) \leq \frac{1}{36} \sum_{\substack{e \in \mathcal{T}_h \\ A(\psi)>0}} \left(\frac{\nabla \psi}{A(\psi)}, \nabla \psi \right)_e, \tag{4.6}$$

$$\left(\frac{|\nabla \phi|^2}{36(A(\phi))^2}, \psi \right) - \left(\frac{\nabla \phi}{18A(\phi)}, \nabla \psi \right) \leq \left(\frac{|\nabla \phi|^2}{18(A(\phi))^2}, A(\psi) \right) + \frac{1}{36} \sum_{\substack{e \in \mathcal{T}_h \\ A(\psi)>0}} \left(\frac{\nabla \psi}{A(\psi)}, \nabla \psi \right)_e. \tag{4.7}$$

Lemma 4.3. For any $\phi \in S_h$, if $A(\phi) > 0$ on one element $e \in \mathcal{T}_h$ with mesh size h_e, then we have

$$\frac{|\nabla \phi|}{A(\phi)} \leq \frac{3\sqrt{2}h_e}{2\triangle_e} \tag{4.8}$$

on the element e.

Proof. Let $P_i = (x_i, y_i)$ $(i = 1, 2, 3)$ be the three vertex points of e, then

$$\frac{\partial \phi}{\partial x} = \frac{1}{2\triangle_e}(\phi(P_1)(y_2 - y_3) + \phi(P_2)(y_3 - y_1) + \phi(P_3)(y_1 - y_2)),$$

$$\frac{\partial \phi}{\partial y} = \frac{1}{2\triangle_e}(\phi(P_1)(x_3 - x_2) + \phi(P_2)(x_1 - x_3) + \phi(P_3)(x_2 - x_1)).$$

So $\nabla\phi$ can be bounded by

$$|\nabla\phi| \leq \frac{\sqrt{2}h_e}{2\triangle_e}(\phi(P_1) + \phi(P_2) + \phi(P_3)).$$

Note that

$$A(\phi) = \frac{1}{3}\left(\phi(P_1) + \phi(P_2) + \phi(P_3)\right),$$

then the lemma is proved. $\qquad\square$

Subsequently, a combination of Lemma 4.2 and Lemma 4.3 leads to the following result.

Lemma 4.4. *Let* $\phi, \psi \in S_h$ *and* $A(\psi) \geq 0$, *then*

$$\left(-\frac{|\nabla\phi|^2}{36(A(\phi))^2}, \psi\right) + \left(\frac{\nabla\phi}{18A(\phi)}, \nabla\psi\right) \leq \frac{C_{\mathcal{T}}}{8}\sum_{e\in\mathcal{T}_h} A(\psi)|_e, \tag{4.9}$$

$$\left(\frac{|\nabla\phi|^2}{36(A(\phi))^2}, \psi\right) - \left(\frac{\nabla\phi}{18A(\phi)}, \nabla\psi\right) \leq \frac{3C_{\mathcal{T}}}{8}\sum_{e\in\mathcal{T}_h} A(\psi)|_e. \tag{4.10}$$

Proof. By Lemma 4.3 and noticing that $A(\psi)$ is constant on every element e, we get

$$\frac{1}{36}\sum_{\substack{e\in\mathcal{T}_h \\ A(\psi)>0}}\left(\frac{\nabla\psi}{A(\psi)}, \nabla\psi\right) = \frac{1}{36}\sum_{\substack{e\in\mathcal{T}_h \\ A(\psi)>0}}\left(\frac{|\nabla\psi|^2}{(A(\psi))^2}, A(\psi)\right) \leq \frac{1}{36}\sum_{e\in\mathcal{T}_h}\frac{9h_e^2}{2\triangle_e^2}(A(\psi), 1)_e = \frac{1}{8}\sum_{e\in\mathcal{T}_h}\frac{h_e^2}{\triangle_e}A(\psi)|_e.$$

Similarly,

$$\left(\frac{|\nabla\phi|^2}{18(A(\phi))^2}, A(\psi)\right) \leq \frac{1}{4}\sum_{e\in\mathcal{T}_h}\frac{h_e^2}{\triangle_e}A(\psi)|_e.$$

Since the element is shape regular, $\frac{h_e^2}{\triangle_e} \leq C_{\mathcal{T}}$, now the lemma is proved by using Lemma 4.2 and Remark 4.1. $\qquad\square$

Theorem 4.1. *Given* $\phi_1^n, \phi_2^n \in S_h$, *with* $0 < \phi_1^n, \phi_2^n < 1$, $0 < \phi_1^n + \phi_2^n < 1$, *(so that* $0 < \overline{\phi_1^n}, \overline{\phi_2^n} < 1$*), there exists a unique solution* $\phi_1^{n+1}, \phi_2^{n+1} \in S_h$ *to (3.17), with* $\overline{\phi_1^{n+1}} = \overline{\phi_1^n}$, $\overline{\phi_2^{n+1}} = \overline{\phi_2^n}$, $0 < \phi_1^{n+1}, \phi_2^{n+1} < 1$, *and* $0 < \phi_1^{n+1} + \phi_2^{n+1} < 1$.

Proof. It is observed that, the numerical solution of (3.17) is a minimizer of the following discrete energy functional with respect to ϕ_1 and ϕ_2

$$\begin{aligned}
\mathcal{J}_h^n(\phi_1, \phi_2) &= \frac{1}{2D_1\tau}\|\phi_1 - \phi_1^n\|_{-1,Q}^2 + \frac{1}{2D_2\tau}\|\phi_2 - \phi_2^n\|_{-1,Q}^2 + (S(\phi_1, \phi_2), 1)_Q \\
&\quad + (\tilde{K}(\phi_1, \phi_2), 1) + (\delta_{\phi_1}H(\phi_1^n, \phi_2^n), \phi_1)_Q + (\delta_{\phi_2}H(\phi_1^n, \phi_2^n), \phi_2)_Q,
\end{aligned} \tag{4.11}$$

over the admissible set

$$\begin{aligned}
A_h := \{(\phi_1, \phi_2) \in S_h \times S_h \mid \phi_1, \phi_2 \geq 0, 0 \leq \phi_1 + \phi_2 \leq 1, \\
\left(\phi_1 - \bar{\phi}_1^0, 1\right)_Q = 0, \quad \left(\phi_2 - \bar{\phi}_2^0, 1\right)_Q = 0\} \subset \mathbb{R}^{2N_p^2}.
\end{aligned} \tag{4.12}$$

It is easy to observe that $\mathcal{J}_h^n$ is a strictly convex functional with respect to ϕ_1 and ϕ_2 over this domain. Consider the following closed domain:

$$\begin{aligned}
A_{h,\delta} := \{(\phi_1, \phi_2) \in S_h \times S_h \mid \phi_1, \phi_2 \geq g(\delta), \delta \leq \phi_1 + \phi_2 \leq 1 - \delta, \\
\left(\phi_1 - \bar{\phi}_1^0, 1\right)_Q = 0, \left(\phi_2 - \bar{\phi}_2^0, 1\right)_Q = 0\} \subset \mathbb{R}^{2N_p^2}.
\end{aligned} \tag{4.13}$$

Since $A_{h,\delta}$ is a bounded, compact and convex set in the following hyperplane V in $\mathbb{R}^{2N_p^2}$, with dimension $2N_p^2 - 2$:

$$V = \left\{(\phi_1, \phi_2) : \frac{1}{|\Omega|}(\phi_1, 1)_Q = \overline{\phi_1^0}, \ \frac{1}{|\Omega|}(\phi_2, 1)_Q = \overline{\phi_2^0}\right\}, \tag{4.14}$$

11

there exists a (may not unique) minimizer of $\mathcal{J}_h^n(\phi_1, \phi_2)$ over $A_{h,\delta}$. The key point of the positivity analysis is that, such a minimizer could not occur on the boundary points (in V) if δ and $g(\delta)$ are small enough.

Assume the minimizer of $\mathcal{J}_h^n(\phi_1, \phi_2)$ occurs at a boundary point of $A_{h,\delta}$.

Case 1: We set the minimization point as $(\phi_1^\star, \phi_2^\star)$, with $\phi_1^\star(P_{\alpha_0}) := \phi_{1,\alpha_0}^\star = g(\delta)$. In addition, we assume that $\phi_1^\star$ reaches the maximum value at α_1, so it is obvious that $\phi_{1,\alpha_1}^\star \geq \overline{\phi_1^\star} = \overline{\phi_1^0}$. We can view the variable ϕ_{1,α_1} as the N_p^2-th one in the hyperplane V, with the condition

$$\phi_{1,\alpha_1} = \frac{(\overline{\phi_1^0}, 1)_Q - \sum_{i \neq \alpha_1}^{N_p}(\phi_{1,i}, \chi_i)_Q}{(\chi_{\alpha_1}, 1)_Q}. \tag{4.15}$$

In more details, we denote the following alternate function

$$\mathcal{U}_h^n\left((\phi_{1,i})|_{i \neq \alpha_1}, \phi_2\right) := \mathcal{J}_h^n\left(\cdot, (\phi_1)_{\alpha_1}, \phi_2\right) = \mathcal{J}_h^n\left(\cdot, \frac{(\overline{\phi_1^0}, 1)_Q - \sum_{i \neq \alpha_1}^{N_p}(\phi_{1,i}, \chi_i)_Q}{(\chi_{\alpha_1}, 1)_Q}, \phi_2\right). \tag{4.16}$$

By a careful calculation, we obtain the following directional derivative

$$\begin{aligned} d_s \mathcal{U}_h^n\left(\phi_1^* + s\psi, \phi_2^\star\right)|_{s=0} = &\frac{1}{D_1\tau}\left(-\Delta_h^{-1}\left(\phi_1^\star - \phi_1^n\right), \psi\right)_Q + \left(\delta_{\phi_1} S\left(\phi_1^\star, \phi_2^\star\right), \psi\right)_Q \\ &+ \left(\delta_{\phi_1}\tilde{K}\left(\phi_1^\star, \phi_2^\star\right), \psi\right) + \left(\delta_{\phi_1}H\left(\phi_1^n, \phi_2^n\right), \psi\right)_Q, \quad \forall\psi \in \mathring{S}_h. \end{aligned} \tag{4.17}$$

This time, due to $(\phi_1^* + s\psi, \phi_2^\star) \in A_{h,\delta}$, let us pick the direction

$$\psi = \delta_{\alpha_0} - C_2\delta_{\alpha_1}, \quad C_2 = \frac{\text{area}(D_{\alpha_0})}{\text{area}(D_{\alpha_1})}, \tag{4.18}$$

where δ_{α_0} and δ_{α_1} are the basis functions on P_{α_0} and P_{α_1}, D_{α_0} and D_{α_1} are the support of δ_{α_0} and δ_{α_1}, respectively.

For the first term appearing in (4.17), an application of Lemma 4.1 gives

$$\begin{aligned} \frac{1}{D_1\tau}(-\Delta_h^{-1}(\phi_1^\star - \phi_1^n), \psi)_Q &= \frac{1}{D_1\tau}\sum_{e \in \mathcal{T}_h}\frac{\triangle_e}{3}\sum_{j=1}^3(-\Delta_h^{-1})(\phi_1^\star - \phi_1^n)\psi(P_{e,j}) \tag{4.19} \\ &= \frac{1}{3D_1\tau}(\text{area}(D_{\alpha_0})(-\Delta_h^{-1})(\phi_1^\star - \phi_1^n)|_{\alpha_0} - C_2\,\text{area}(D_{\alpha_1})(-\Delta_h^{-1})(\phi_1^\star - \phi_1^n)|_{\alpha_1}) \\ &= \frac{1}{3D_1\tau}\text{area}(D_{\alpha_0})\left((-\Delta_h^{-1})(\phi_1^\star - \phi_1^n)|_{\alpha_0} - (-\Delta_h^{-1})(\phi_1^\star - \phi_1^n)|_{\alpha_1}\right) \\ &\leq \frac{2C_1}{3D_1\tau}\text{area}(D_{\alpha_0}). \end{aligned}$$

For the second term, we see that

$$\begin{aligned} (\delta_{\phi_1}S(\phi_1^\star, \phi_2^\star), \psi)_Q &= \left(\frac{1}{\gamma}\ln(\frac{\alpha\phi_1^\star}{\gamma}) - \ln(1 - \phi_1^\star - \phi_2^\star), \psi\right)_Q \tag{4.20} \\ &= \sum_{e \in \mathcal{T}_h}\left(\frac{1}{3}\triangle_e\sum_{j=1}^3\left(\frac{1}{\gamma}\ln(\frac{\alpha\phi_1^\star}{\gamma}) - \ln(1 - \phi_1^\star - \phi_2^\star)\right)\psi(P_{e,j})\right) \\ &= \frac{1}{3}\text{area}(D_{\alpha_0})\left(\left(\frac{1}{\gamma}\ln(\frac{\alpha\phi_1^\star}{\gamma}) - \ln(1 - \phi_1^\star - \phi_2^\star)\right)|_{\alpha_0}\right. \\ &\quad \left. - \left(\frac{1}{\gamma}\ln(\frac{\alpha\phi_1^\star}{\gamma}) - \ln(1 - \phi_1^\star - \phi_2^\star)\right)|_{\alpha_1}\right) \\ &= \frac{1}{3}\text{area}(D_{\alpha_0})\left(\ln\frac{(\phi_1^\star)^{\frac{1}{\gamma}}}{1 - \phi_1^\star - \phi_2^\star}|_{\alpha_0} - \ln\frac{(\phi_1^\star)^{\frac{1}{\gamma}}}{1 - \phi_1^\star - \phi_2^\star}|_{\alpha_1}\right) \\ &\leq \frac{1}{3}\text{area}(D_{\alpha_0})\left(\ln\frac{(g(\delta))^{\frac{1}{\gamma}}}{\delta} - \ln\frac{(\bar{\phi}_1^0)^{\frac{1}{\gamma}}}{1 - \delta}\right) \end{aligned}$$

$$\leq \frac{1}{3} \operatorname{area}(D_{\alpha_0}) \left(\ln \frac{(g(\delta))^{\frac{1}{\gamma}}}{\delta} - \ln(\bar{\phi}_1^0)^{\frac{1}{\gamma}} \right).$$

For the third term, we have

$$\left(\delta_{\phi_1} \tilde{K} \left(\phi_1^\star, \phi_2^\star\right), \psi\right) = \left(-\frac{a_1^2 |\nabla \phi_1^\star|^2}{36(A(\phi_1^\star))^2}, \psi\right) + \left(\frac{a_1^2 \nabla \phi_1^\star}{18 A(\phi_1^\star)}, \nabla \psi\right) \tag{4.21}$$

$$+ \left(\frac{a_3^2 |\nabla (1 - \phi_1^\star - \phi_2^\star)|^2}{36 \left(A(1 - \phi_1^\star - \phi_2^\star)\right)^2}, \psi\right) - \left(\frac{a_3^2 \nabla (1 - \phi_1^\star - \phi_2^\star)}{18 A (1 - \phi_1^\star - \phi_2^\star)}, \nabla \psi\right).$$

By Lemma 4.4,

$$\left(-\frac{a_1^2 |\nabla \phi_1^\star|^2}{36(A(\phi_1^\star))^2}, \psi\right) + \left(\frac{a_1^2 \nabla \phi_1^\star}{18 A(\phi_1^\star)}, \nabla \psi\right) \leq \frac{a_1^2 C_{\mathcal{T}}}{8} \sum_{e \in \mathcal{T}_h} A(\delta_{\alpha_0})|_e + \frac{3 a_1^2 C_2 C_{\mathcal{T}}}{8} \sum_{e \in \mathcal{T}_h} A(\delta_{\alpha_1})|_e \tag{4.22}$$

$$= \frac{a_1^2 C_{\mathcal{T}}}{24} \sum_{e \in D_{\alpha_0}} 1 + \frac{a_1^2 C_2 C_{\mathcal{T}}}{8} \sum_{e \in D_{\alpha_1}} 1.$$

Similarly,

$$\left(\frac{a_3^2 |\nabla (1 - \phi_1^\star - \phi_2^\star)|^2}{36 \left(A(1 - \phi_1^\star - \phi_2^\star)\right)^2}, \psi\right) - \left(\frac{a_3^2 \nabla (1 - \phi_1^\star - \phi_2^\star)}{18 A (1 - \phi_1^\star - \phi_2^\star)}, \nabla \psi\right) \leq \frac{a_3^2 C_{\mathcal{T}}}{8} \sum_{e \in D_{\alpha_0}} 1 + \frac{a_3^2 C_2 C_{\mathcal{T}}}{24} \sum_{e \in D_{\alpha_1}} 1. \tag{4.23}$$

Then the term $\delta_{\phi_1} \tilde{K}$ can be bounded by

$$\left(\delta_{\phi_1} \tilde{K} \left(\phi_1^\star, \phi_2^\star\right), \psi\right) \leq \frac{(a_1^2 + 3 a_3^2) C_{\mathcal{T}}}{24} \sum_{e \in D_{\alpha_0}} 1 + \frac{(3 a_1^2 + a_3^2) C_2 C_{\mathcal{T}}}{24} \sum_{e \in D_{\alpha_1}} 1. \tag{4.24}$$

For the numerical solution ϕ_1^n at the previous time step, the a-priori assumption $0 < \phi_1^n < 1$ indicates that

$$-1 \leq \phi_1^n(P_{\alpha_0}) - \phi_1^n(P_{\alpha_1}) \leq 1.$$

For the last term, we have

$$\left(\delta_{\phi_1} H \left(\phi_1^n, \phi_2^n\right), \psi\right)_Q = (\chi_{13} - 2\chi_{13}\phi_1^n + (\chi_{12} - \chi_{13} - \chi_{23})\phi_2, \psi)_Q \tag{4.25}$$

$$= \sum_{e \in \mathcal{T}_h} \frac{1}{3} \triangle_e \left(\sum_{j=1}^{3} (\chi_{13} - 2\chi_{13}\phi_1^n - (\chi_{12} - \chi_{13} - \chi_{23})\phi_2^n)\psi(P_{e,j}) \right)$$

$$= \frac{1}{3} \operatorname{area}(D_{\alpha_0}) \left(-2\chi_{13}(\phi_1^n|_{\alpha_0} - \phi_1^n|_{\alpha_1}) - (\chi_{12} - \chi_{13} - \chi_{23})(\phi_2^n|_{\alpha_0} - \phi_2^n|_{\alpha_1}) \right)$$

$$\leq \frac{1}{3} \operatorname{area}(D_{\alpha_0})(\chi_{12} + 3\chi_{13} + \chi_{23}).$$

To sum up, the following inequality is available

$$d_s \mathcal{U}_h^n \left(\phi_1^* + s\psi, \phi_2^\star\right)|_{s=0} \leq \frac{1}{3} \operatorname{area}(D_{\alpha_0}) \ln \frac{(g(\delta))^{\frac{1}{\gamma}}}{\delta} + r_0, \tag{4.26}$$

in which $r_0 = \frac{\operatorname{area}(D_{\alpha_0})}{3} \left(\frac{2 C_1}{D_1 \tau} - \ln(\bar{\phi}_1^0)^{\frac{1}{\gamma}} + \chi_{12} + 3\chi_{13} + \chi_{23}\right) + \frac{(a_1^2 + 3 a_3^2) C_{\mathcal{T}}}{24} \sum_{e \in D_{\alpha_0}} 1 + \frac{(3 a_1^2 + a_3^2) C_2 C_{\mathcal{T}}}{24} \sum_{e \in D_{\alpha_1}} 1$. Note that r_0 is a constant for a fixed τ, h, while it becomes singular as $\tau \longrightarrow 0$. For any fixed τ, we could choose $g(\delta)$ sufficiently small so that

$$\frac{1}{3} \operatorname{area}(D_{\alpha_0}) \ln \frac{(g(\delta))^{\frac{1}{\gamma}}}{\delta} + r_0 < 0, \tag{4.27}$$

such as $g(\delta) = \left(\delta \exp\left(-\frac{3(r_0+1)}{\operatorname{area}(D_{\alpha_0})}\right) \right)^\gamma$. This in turn shows that

$$d_s \mathcal{U}_h^n \left(\phi_1^\star + s\psi, \phi_2^\star\right)|_{s=0} < 0, \text{ for } g(\delta) \text{ satisfying } (4.27).$$

13

This contradicts the assumption that $\mathcal{J}_h^n$ has a minimum at $(\phi_1^\star, \phi_2^\star)$, since the directional derivative is negative in a direction pointing into $(A_{h,\delta})^\circ$, the interior of $A_{h,\delta}$.

Case 2: Using similar arguments as in Case 1, we can also prove that, the global minimum of $\mathcal{J}_h^n$ over $A_{h,\delta}$ could not occur on the boundary section of $\phi_{2,\alpha_0} = g(\delta)$, for any grid node number α_0, if $g(\delta)$ is small enough.

Case 3: We set the minimization point as $(\phi_1^\star, \phi_2^\star)$, with $\phi_{1,\alpha_0}^\star + \phi_{2,\alpha_0}^\star = 1 - \delta$, where α_0 represents α_0-th grid node number, and assume that $\phi_{1,\alpha_0} \geq \frac{1}{3}$. In addition, $(\phi_1 + \phi_2, 1) = \overline{\phi_1^0} + \overline{\phi_2^0}$, there exists one grid point $\alpha_1 = (i_1, j_1)$, so that $\phi_1^\star + \phi_2^\star$ reaches the maximum value. It is obvious that $\phi_{1,\alpha_1}^\star + \phi_{2,\alpha_1}^\star \leq \overline{\phi_1^\star} + \overline{\phi_2^\star} = \overline{\phi_1^0} + \overline{\phi_2^0}$. Similarly, the variable ϕ_{1,α_1} could be viewed as the N_p^2-th one in the hyperplane V, with the condition

$$\phi_{1,\alpha_1} = \frac{(\overline{\phi_1^0}, 1)_Q - \sum_{i \neq \alpha_1}^{N_p}(\phi_{1,i}, \chi_i)_Q}{(\chi_{\alpha_1}, 1)_Q}. \tag{4.28}$$

In more details, the following alternate function is introduced

$$\mathcal{U}_h^n\left((\phi_{1,i})|_{i \neq \alpha_1}, \phi_2\right) := \mathcal{J}_h^n\left(\cdot, (\phi_1)_{\alpha_1}, \phi_2\right) = \mathcal{J}_h^n\left(\cdot, \frac{(\overline{\phi_1^0}, 1)_Q - \sum_{i \neq \alpha_1}^{N_p}(\phi_{1,i}, \chi_i)_Q}{(\chi_{\alpha_1}, 1)_Q}, \phi_2\right). \tag{4.29}$$

Again, a careful calculation implies the following directional derivative

$$d_s\mathcal{U}_h^n\left(\phi_1^* + s\psi, \phi_2^\star\right)|_{s=0} = \frac{1}{D_1\tau}\left(-\Delta_h^{-1}\left(\phi_1^\star - \phi_1^n\right), \psi\right)_Q + \left(\delta_{\phi_1}S\left(\phi_1^\star, \phi_2^\star\right), \psi\right)_Q$$
$$+ \left(\delta_{\phi_1}\tilde{K}\left(\phi_1^\star, \phi_2^\star\right), \psi\right) + \left(\delta_{\phi_1}H\left(\phi_1^n, \phi_2^\star\right), \psi\right)_Q, \quad \forall\psi \in \mathring{S}_h. \tag{4.30}$$

In this case, since $(\phi_1^* + s\psi, \phi_2^\star) \in A_{h,\delta}$, we pick the direction

$$\psi = C_2\delta_{\alpha_1} - \delta_{\alpha_0}, C_2 = \frac{\text{area}(D_{\alpha_0})}{\text{area}(D_{\alpha_1})}. \tag{4.31}$$

For the first term in (4.30), an application of Lemma 4.1 leads to

$$\frac{1}{D_1\tau}(-\Delta_h^{-1}(\phi_1^\star - \phi_1^n), \psi)_Q = \frac{1}{D_1\tau}\sum_{e \in \mathcal{T}_h}\frac{1}{3}\triangle_e\sum_{j=1}^{3}\Delta_h^{-1}(\phi_1^\star - \phi_1^n)\psi(P_{e,j}) \tag{4.32}$$

$$= \frac{1}{3D_1\tau}(C_2\,\text{area}(D_{\alpha_1})(-\Delta_h^{-1})(\phi_1^\star - \phi_1^n)|_{\alpha_1} - \text{area}(D_{\alpha_0})(-\Delta_h^{-1})(\phi_1^\star - \phi_1^n)|_{\alpha_0})$$

$$= \frac{1}{3D_1\tau}\,\text{area}(D_{\alpha_0})\left((-\Delta_h^{-1})(\phi_1^\star - \phi_1^n)|_{\alpha_1} - (-\Delta_h^{-1})(\phi_1^\star - \phi_1^n)|_{\alpha_0}\right)$$

$$\leq \frac{2C_1}{3D_1\tau}\,\text{area}(D_{\alpha_0}).$$

For the second term, a similar inequality could be derived

$$(\delta_{\phi_1}S(\phi_1^\star, \phi_2^\star), \psi)_Q = \left(\frac{1}{\gamma}\ln(\frac{\alpha\phi_1^\star}{\gamma}) - \ln(1 - \phi_1^\star - \phi_2^\star), \psi\right)_Q \tag{4.33}$$

$$= \sum_{e \in \mathcal{T}_h}\left(\frac{1}{3}\triangle_e\sum_{j=1}^{3}\left(\frac{1}{\gamma}\ln(\frac{\alpha\phi_1^\star}{\gamma}) - \ln(1 - \phi_1^\star - \phi_2^\star)\right)\psi(P_{e,j})\right)$$

$$= -\frac{1}{3}\,\text{area}(D_{\alpha_0})\left(\left(\frac{1}{\gamma}\ln(\frac{\alpha\phi_1^\star}{\gamma}) - \ln(1 - \phi_1^\star - \phi_2^\star)\right)|_{\alpha_1}\right.$$

$$\left. - \left(\frac{1}{\gamma}\ln(\frac{\alpha\phi_1^\star}{\gamma}) - \ln(1 - \phi_1^\star - \phi_2^\star)\right)|_{\alpha_0}\right)$$

$$= -\frac{1}{3}\,\text{area}(D_{\alpha_0})\left(\ln\frac{(\phi_1^\star)^{\frac{1}{\gamma}}}{1 - \phi_1^\star - \phi_2^\star}|_{\alpha_1} - \ln\frac{(\phi_1^\star)^{\frac{1}{\gamma}}}{1 - \phi_1^\star - \phi_2^\star}|_{\alpha_0}\right)$$

14

$$\leq \frac{1}{3}\,\mathrm{area}(D_{\alpha_0})\left(\ln\frac{1}{1-\bar\phi_1^0-\bar\phi_2^0}-\ln\frac{\frac{1}{3}^{1/\gamma}}{\delta}\right).$$

For the third term, we have the following expansion as in (4.24):

$$\left(\delta_{\phi_1}\tilde K\left(\phi_1^\star,\phi_2^\star\right),\psi\right)\leq \frac{(3a_1^2+a_3^2)C_{\mathcal T}}{24}\sum_{e\in D_{\alpha_0}}1+\frac{(a_1^2+3a_3^2)C_2C_{\mathcal T}}{24}\sum_{e\in D_{\alpha_1}}1. \tag{4.34}$$

For the last term in (4.30), since the numerical solution at the previous time step is involved, the a-priori assumption $0<\phi_1^n<1$ indicates that

$$-1\leq \phi_{1,\alpha_0}^n-\phi_{1,\alpha_1}^n\leq 1,$$

which in turn results in the following inequality

$$\left(\delta_{\phi_1}H\left(\phi_1^n,\phi_2^n\right),\psi\right)_Q=(\chi_{13}-2\chi_{13}\phi_1^n+(\chi_{12}-\chi_{13}-\chi_{23})\phi_2,\psi)_Q \tag{4.35}$$

$$=\sum_{e\in\mathcal T_h}\frac{1}{3}\triangle_e\left(\sum_{j=1}^3(\chi_{13}-2\chi_{13}\phi_1^n-(\chi_{12}-\chi_{13}-\chi_{23})\phi_2^n)\psi(P_{e,j})\right)$$

$$=\frac{1}{3}\,\mathrm{area}(D_{\alpha_0})\left(-2\chi_{13}(\phi_1^n|_{\alpha_1}-\phi_1^n|_{\alpha_0})-(\chi_{12}-\chi_{13}-\chi_{23})(\phi_2^n|_{\alpha_1}-\phi_2^n|_{\alpha_0})\right)$$

$$\leq\frac{1}{3}\,\mathrm{area}(D_{\alpha_0})(\chi_{12}+3\chi_{13}+\chi_{23}).$$

In turn, a summation of the above estimates yields

$$d_s\mathcal U_h^n\left(\phi_1^*+s\psi,\phi_2^\star\right)|_{s=0}\leq\frac{1}{3}\,\mathrm{area}(D_{\alpha_0})\ln\delta+r_1, \tag{4.36}$$

in which $r_1=\frac{1}{3}\,\mathrm{area}(D_{\alpha_0})(\frac{2C_1}{D_1\tau}+\frac{1}{\gamma}\ln 3+\ln\frac{1}{1+\bar\phi_1^0+\bar\phi_2^0}+\chi_{12}+3\chi_{13}+\chi_{23})+\frac{(3a_1^2+a_3^2)C_{\mathcal T}}{24}\sum_{e\in D_{\alpha_0}}1+\frac{(a_1^2+3a_3^2)C_2C_{\mathcal T}}{24}\sum_{e\in D_{\alpha_1}}1$. Again, r_1 is a constant for a fixed τ and h, we could choose δ sufficiently small so that

$$\frac{1}{3}\,\mathrm{area}(D_{\alpha_0})\ln\delta+r_1<0, \tag{4.37}$$

such as $\delta=\exp\left(-\frac{3(r_1+1)}{\mathrm{area}(D_{\alpha_0})}\right)$. This in turn demonstrates that

$$d_s\mathcal U_h^n\left(\phi_1^\star+s\psi,\phi_2^\star\right)|_{s=0}<0,\ \text{for }g(\delta)\text{ satisfy (4.37)},$$

which contradicts the assumption that $\mathcal J_h^n$ has a minimum at $(\phi_1^\star,\phi_2^\star)$, since the directional derivative is negative in a direction pointing into $(A_{h,\delta})^\circ$, the interior of $A_{h,\delta}$.

Case 4: Using similar arguments, we can also prove that, the global minimum of $\mathcal J_h^n$ over $\mathcal A_{h,\delta}$ could not occur on the boundary section where $\phi_{1,\alpha_0}^\star+\phi_{2,\alpha_0}^\star=1-\delta$, if δ is sufficiently small, for any point index α_0. The details are left to the interested readers.

Finally, a combination of these four cases shows that, the global minimizer of $\mathcal J_h^n(\phi_1,\phi_2)$ could only possibly occur at interior point of $(A_{h,\delta})^0\subset(A_h)^0$. We conclude that there must be a solution $(\phi_1,\phi_2)\in(A_h)^0$ that minimizes $\mathcal J_h^n(\phi_1,\phi_2)$ over A_h, which is equivalent to the numerical solution of (3.17). The existence of the numerical solution is established.

In addition, since $\mathcal J_h^n(\phi_1,\phi_2)$ is a strictly convex function over A_h, the uniqueness analysis for this numerical solution is straightforward. The proof of Theorem 4.1 is complete. $\square$

5. The energy stability

An unconditional energy stability for the proposed numerical scheme (3.17) is stated below.

Theorem 5.1. *(energy stability) The unique solution of the mass lumped fully-discrete scheme* (3.17) *is unconditionally energy stable, i.e., for any time step size $\tau>0$, the following estimate is valid:*

$$\hat E(\phi_{1h}^{n+1},\phi_{2h}^{n+1})\leq\hat E(\phi_{1h}^n,\phi_{2h}^n). \tag{5.1}$$

Proof. The energy stability of the mass lumped scheme (3.17) is a direct consequence of Lemma 3.4.

For $w_1, w_2 \in \mathring{S}_h$, we denote $v_1 = (-\Delta_h)^{-1}w_1, v_2 = (-\Delta_h)^{-1}w_2$, and obtain

$$
\begin{aligned}
&\left(\frac{\phi_{1h}^{n+1} - \phi_{1h}^n}{D_1\tau}, (-\Delta_h)^{-1}w_1\right)_Q + \left(\delta_{\phi_1}\tilde{K}(\phi_{1h}^{n+1}, \phi_{2h}^{n+1}), w_1\right) \\
&\qquad + \left(\frac{\partial}{\partial\phi_1}S(\phi_{1h}^{n+1}, \phi_{2h}^{n+1}) + \frac{\partial}{\partial\phi_1}H(\phi_{1h}^{n+1}, \phi_{2h}^{n+1}), w_1\right)_Q = 0, \\
&\left(\frac{\phi_{2h}^{n+1} - \phi_{2h}^n}{D_2\tau}, (-\Delta_h)^{-1}w_2\right)_Q + \left(\delta_{\phi_2}\tilde{K}(\phi_{1h}^{n+1}, \phi_{2h}^{n+1}), w_2\right) \\
&\qquad + \left(\frac{\partial}{\partial\phi_2}S(\phi_{1h}^{n+1}, \phi_{2h}^{n+1}) + \frac{\partial}{\partial\phi_2}H(\phi_{1h}^{n+1}, \phi_{2h}^{n+1}), w_2\right)_Q = 0.
\end{aligned}
\tag{5.2}
$$

In turn, by setting $w_1 = \phi_{1h}^{n+1} - \phi_{1h}^n, w_2 = \phi_{2h}^{n+1} - \phi_{2h}^n$, and applying Lemma 3.4, we arrive at

$$
\begin{aligned}
0 &= \frac{1}{D_1\tau}\|\phi_{1h}^{n+1} - \phi_{1h}^n\|_{-1,Q}^2 + \left(\frac{\partial}{\partial\phi_1}S(\phi_{1h}^{n+1}, \phi_{2h}^{n+1}) + \frac{\partial}{\partial\phi_1}H(\phi_{1h}^{n+1}, \phi_{2h}^{n+1}), \phi_{1h}^{n+1} - \phi_{1h}^n\right)_Q \\
&+ \frac{1}{D_2\tau}\|\phi_{2h}^{n+1} - \phi_{2h}^n\|_{-1,Q}^2 + \left(\frac{\partial}{\partial\phi_2}S(\phi_{1h}^{n+1}, \phi_{2h}^{n+1}) + \frac{\partial}{\partial\phi_2}H(\phi_{1h}^{n+1}, \phi_{2h}^{n+1}), \phi_{2h}^{n+1} - \phi_{2h}^n\right)_Q \\
&+ \left(\delta_{\phi_1}\tilde{K}(\phi_{1h}^{n+1}, \phi_{2h}^{n+1}), \phi_{1h}^{n+1} - \phi_{1h}^n\right) + \left(\delta_{\phi_2}\tilde{K}(\phi_{1h}^{n+1}, \phi_{2h}^{n+1}), \phi_{2h}^{n+1} - \phi_{2h}^n\right) \\
&\geq \frac{1}{D_1\tau}\|\phi_{1h}^{n+1} - \phi_{1h}^n\|_{-1,Q}^2 + \frac{1}{D_2\tau}\|\phi_{2h}^{n+1} - \phi_{2h}^n\|_{-1,Q}^2 + \hat{E}(\phi_{1h}^{n+1}, \phi_{2h}^{n+1}) - \hat{E}(\phi_{1h}^n, \phi_{2h}^n) \\
&\geq \hat{E}(\phi_{1h}^{n+1}, \phi_{2h}^{n+1}) - \hat{E}(\phi_{1h}^n, \phi_{2h}^n).
\end{aligned}
$$

This finishes the proof of Theorem 5.1. $\qquad\qquad\qquad\qquad\qquad\qquad\qquad\qquad\square$

6. Numerical results

In this section, we perform some numerical simulations using the proposed scheme (3.17). In [32], the authors simulated several numerical examples for solving three-component MMC-TDGL equations by the SAV method and showed some phase transition processes, with different initial concentrations as well as the statistical segment lengths $a_i, i = 1, 2, 3$, consistent with an earlier work [34]. The statistical segment lengths a_i in the deGennes interfacial gradient terms, $\frac{1}{36}\sum_{i=1}^3 \frac{a_i^2}{\phi_i}|\nabla\phi_i|^2, i = 1, 2, 3$, determine the interface thickness. Now, the default parameter of MMC-TDGL is selected to make F_e convex; see Table 1. In fact, these parameters are only used for the numerical experiments, to validate the effectiveness of the proposed finite element scheme. In the numerical simulation of more realistic physical problems, these parameters could be easily adjusted, and no essential pattern difference is expected for the computational results with the parameter modification.

Parameter	D_1	D_2	χ_{12}	χ_{13}	χ_{23}	γ	N	a_1	a_2	a_3
Value	1	1	4	10	1.6	0.16	5.12	1	1	1

TABLE 1. The values of the parameters in the simulation

The first example is aimed to test the numerical convergence. The second one simulates a periodic structure on a large domain. In addition, the third one is designed to show some realistic results associated with the evolution of macromolecular microsphere hydrogels. For convenience, we only consider the periodic boundary condition, and the case of homogeneous Neumann boundary condition could be similarly handled.

Example 6.1. *Let parameter $a_1 = a_2 = a_3 = 0.3$, while keeping the other default parameters constant. Consider the MMC-TDGL equation over the domain $\Omega = (0,1)^2$, with the initial data given by*

$$\phi_1(x, y, 0) = 0.1 + 0.01 \cos(2\pi x) \cos(2\pi y),$$
$$\phi_2(x, y, 0) = 0.5 + 0.01 \cos(2\pi x) \cos(2\pi y).$$
(6.1)

We use the triangular mesh with size $h = 1/256$ for partition of the domain. Since the exact solution is unknown, we compute the errors by adjacent time step in the numerical accuracy test. Figure 6.1 presents the L^∞ and L^2 numerical errors of the three-phase variables, ϕ_1, ϕ_2, ϕ_3, as well as a reference line at the terminal time $T = 0.02$. In turn, the time step size is determined by the formula $\tau = \frac{T}{N_T}$, in which N_T stands for the total number of time steps. Due to the $O(h^2)$ approximation in space, the spatial error is negligible. The expected temporal numerical accuracy assumption $e = C\tau$ indicates that $\ln|e| = \ln(CT) - \ln N_T$, so that we plot $\ln|e|$ versus. $\ln N_T$ to demonstrate the temporal convergence order. The reference line has an exact slope of -1, while the least square approximation to the L^2 error curves has approximate slopes -1.0466, -1.0122, -1.0154, for the variables ϕ_1, ϕ_2 and ϕ_3, respectively. In other words, a perfect first order temporal convergence rate is reported.
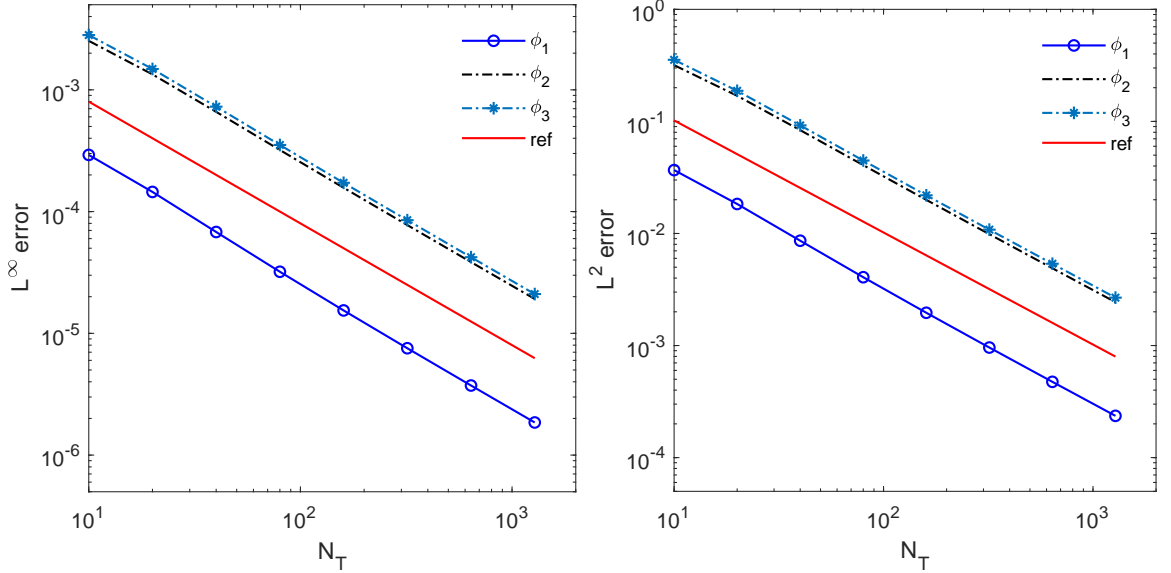
FIGURE 6.1. The L^∞ and L^2 numerical errors versus temporal resolution N_T, at the final time $T = 0.02$ in Example 6.1, by fixing $h = 1/256$. The time step size is given by $\tau = \frac{T}{N_T}$. The reference line has an exact slope of -1, while the least square approximation to the L^2 error curves has approximate slopes -1.0466, -1.0122, -1.0154, for the variables ϕ_1, ϕ_2 and ϕ_3, respectively.

In the accuracy test for the spatial convergence order, we set the time size as $\tau = 7.8125e - 6$, so that the temporal error is negligible. A sequence of spatial resolutions are taken, with $h = \frac{1}{N_0}$. The expected temporal numerical accuracy assumption $e = Ch^2$ indicates that $\ln|e| = \ln C - 2\ln N_0$, so that we plot $\ln|e|$ versus $\ln N_0$ to demonstrate the temporal convergence order. Similarly, Figure 6.2 presents the L^∞ and L^2 numerical errors of the three-phase variables, as well as a reference line at the terminal time $T = 0.02$, for this spatial convergence order test. The reference line has an exact slope of -2, while the least square approximation to the L^2 error curves has approximate slopes -2.0532, -2.0476, -2.0480, for the variables ϕ_1, ϕ_2 and ϕ_3, respectively. Therefore, a perfect second order spatial convergence rate is reported.
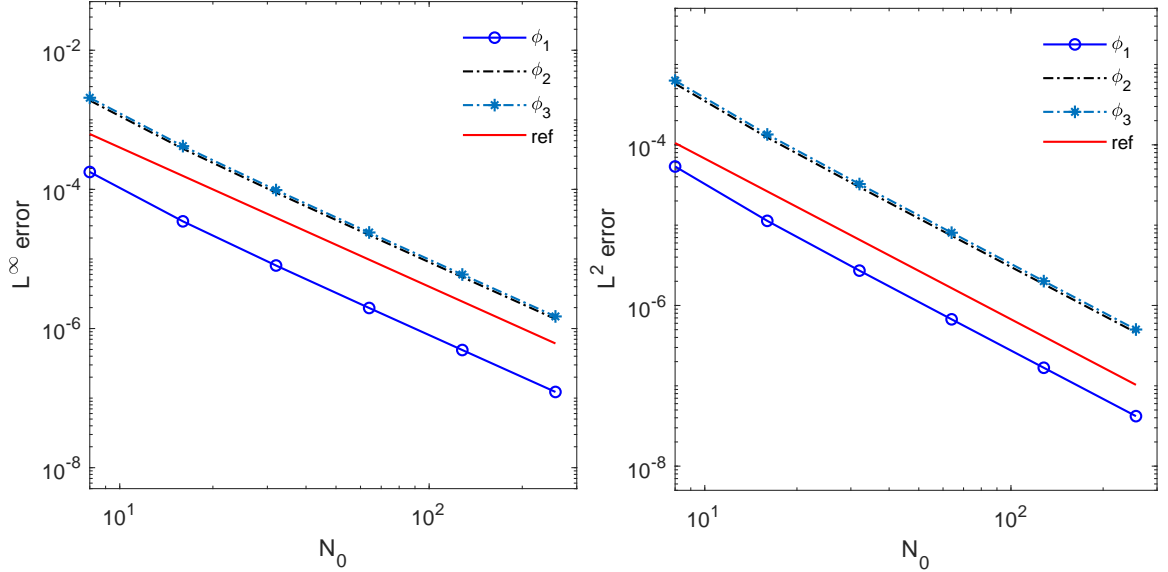
FIGURE 6.2. The L^∞ and L^2 numerical errors versus spatial resolution N_0, at the final time $T = 0.02$ in Example 6.1, by fixing $\tau = 7.8125e - 6$. The spatial mesh size is given by $h = \frac{1}{N_0}$. The reference line has an exact slope of -2, while the least square approximation to the L^2 error curves has approximate slopes -2.0532, -2.0476, -2.0480, for the variables ϕ_1, ϕ_2 and ϕ_3, respectively.

Example 6.2. *Consider the MMC-TDGL equation over the domain $\Omega = (0, 64)^2$, with the initial data given by*

$$\phi_1(x, y, 0) = 0.1 + 0.01 \cos(3\pi x/32) \cos(3\pi y/32),$$
$$\phi_2(x, y, 0) = 0.5 + 0.01 \cos(3\pi x/32) \cos(3\pi y/32). \tag{6.2}$$

We use the triangular mesh with size $h = 1/4$ for partition of the domain, and take the time step size as $\tau = 0.01$. Figure 6.3 displays the configuration of the simulated solution ϕ_2 at a sequence of time instants, t=0, 5, 8, 10, 15 and 20, respectively. It is observed that the phase structures have a drastic change in time, and then asymptotically evolve to a steady state, which is consistent with the energy evolution plotted in Figure 6.7. In addition, the configuration of all three phase variables are presented in Figure 6.4, at a sequence of later time instants, t=25, 80, and 200, respectively. The corresponding evolutions of the mass, as well as the maximum and minimum values of the phase variables, are displayed in Figures 6.5, 6.6, respectively. The mass conservation and the positivity property are observed to be preserved in these evolution figures.

Example 6.3. *Considered the MMC-TDGL equations over the domain $\Omega = (0, 50)^2$, with the initial data given by*

$$\phi_1(x, y, 0) = 0.1 + r_{i,j},$$
$$\phi_2(x, y, 0) = 0.5 + r_{i,j}, \tag{6.3}$$

where the $r_{i,j}$ are uniformly distributed random numbers in $[-0.01, 0.01]$.

We use the uniform triangular mesh with size $h = 1/4$, take the time step size as $\tau = 0.01$, and focus on the ϕ_2 variable, which reflects the polymer chain distribution. In this example, the initial concentration of polymer segments reaches $0.5 + r_{i,j}$, every MMS can be joined by polymer chains since there are enough segments to grow. Thus the reticular structure can be obtained. Figure 6.8 displays the plot of the ϕ_2 variable at a sequence of time instants, t=0, 3.6, 6.52, 8, 10, 26, 85, 278 and 500,
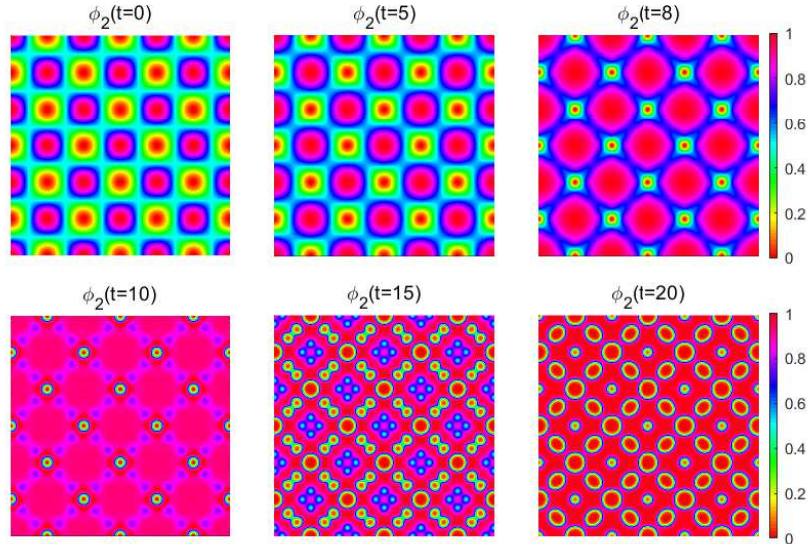
18

FIGURE 6.3. The simulated solution ϕ_2, at t=0, 5, 8, 10, 15 and 20 respectively, in Example 6.2

respectively. It is observed that the red area in the third row becomes larger, that is, the structure is tighter, which is consistent with [32, 34].

The evolution of the corresponding energy is plotted in Figure 6.9, which indicates a monotone decrease in time. Figures 6.10 and 6.11 display the maximum and minimum value of the phase variables and the mass. Again, the positivity-preserving property and mass conversation have been perfectly demonstrated in the numerical simulation.

7. Concluding remarks

In this paper, we have developed a positivity-preserving and energy stable finite element scheme for the three-component Cahn-Hilliard flow model involved in macromolecular microsphere composite hydrogels, with the Flory-Huggins-deGennes energy potential in the ternary system. A convex-concave decomposition of the energy functional in multi-phase space is recalled, which in turn leads to an implicit treatment of the logarithmic and the nonlinear surface diffusion terms, as well as an explicit update of the concave expansive linear terms. In the spatial discretization, the mass lumped finite element approximation is applied. Both the positivity preserving property and the unconditional energy stability are theoretically justified, which will be the first such results for a finite element scheme applied to the ternary MMC system. A few numerical examples are presented, which demonstrate the robustness and accuracy of the proposed numerical scheme.

Declarations

Conflicts of interest/Competing interests: not applicable
Availability of data and material: not applicable
Code availability: not applicable
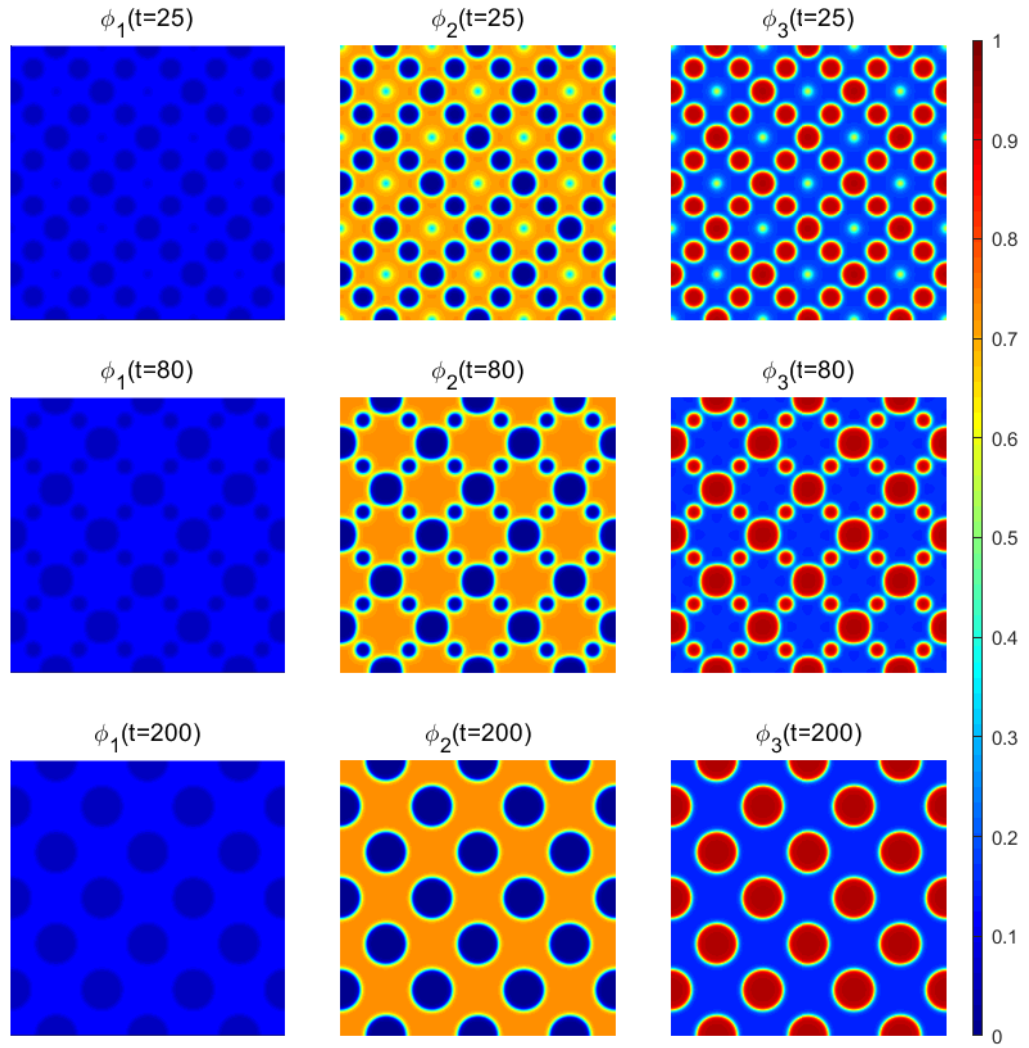**Ethics approval:** not applicable

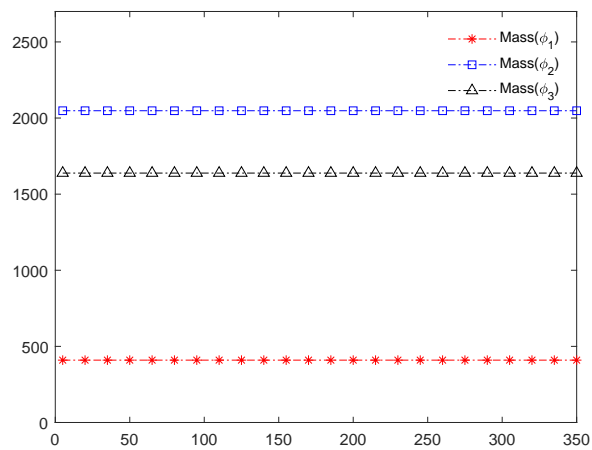FIGURE 6.4. The phase variables plot in Example 6.2, at t=25, 80 and 200

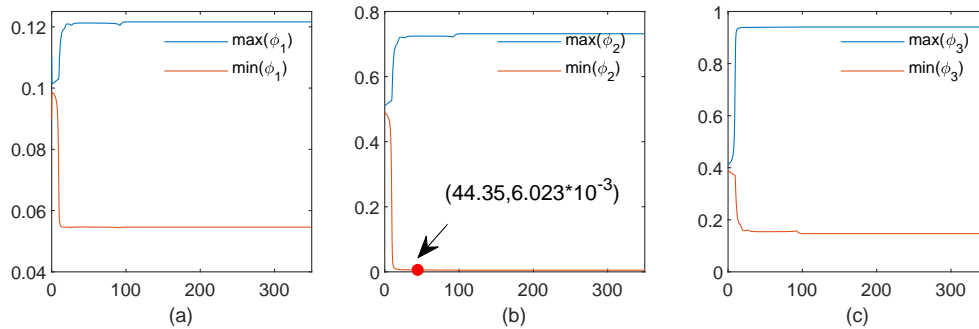FIGURE 6.5. Mass evolution of the phase variables in Example 6.2

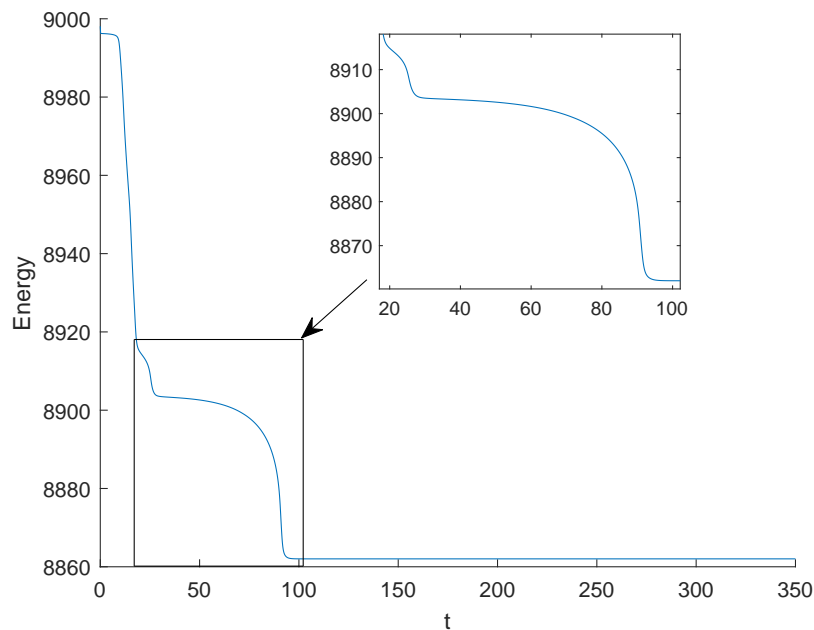FIGURE 6.6. Evolution of the maximum and minimum value of phase variables in Example 6.2

FIGURE 6.7. Energy evolution of the simulated solution in Example 6.2

Consent to participate: not applicable
Consent for publication: not applicable

REFERENCES

[1] H. Abels and M. Wilke. Convergence to equilibrium for the Cahn-Hilliard equation with a logarithmic free energy. *Nonlinear Anal.*, 67:3176–3193, 2007.

[2] A. Baskaran, Z. Hu, J. Lowengrub, C. Wang, S. Wise, and P. Zhou. Energy stable and efficient finite-difference nonlinear multigrid schemes for the modified phase field crystal equation. *J. Comput. Phys.*, 250:270–292, 2013.

[3] A. Baskaran, J. Lowengrub, C. Wang, and S. Wise. Convergence analysis of a second order convex splitting scheme for the modified phase field crystal equation. *SIAM J. Numer. Anal.*, 51:2851–2873, 2013.

[4] F. Boyer and C. Lapuerta. Study of a three component Cahn-Hilliard flow model. *ESAIM Math. Model. Numer. Anal.*, 40(4):653–687, 2006.

[5] F. Boyer and S. Minjeaud. Numerical schemes for a three component Cahn-Hilliard model. *ESAIM Math. Model. Numer. Anal.*, 45(4):697–738, 2011.

[6] W. Chen, S. Conde, C. Wang, X. Wang, and S. Wise. A linear energy stable scheme for a thin film model without slope selection. *J. Sci. Comput.*, 52:546–562, 2012.
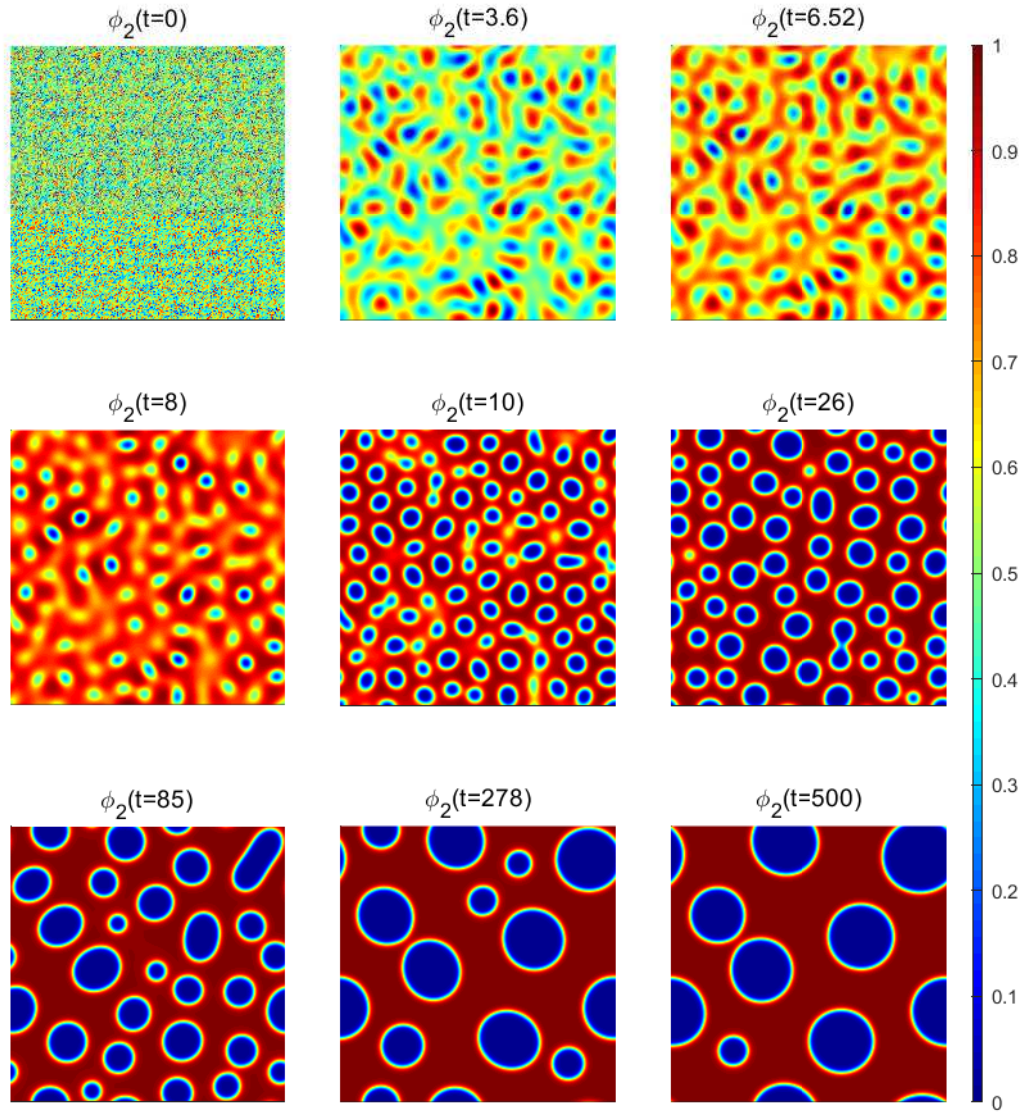
FIGURE 6.8. The phase variable plot for ϕ_2 at a sequence of time instants $t=0$, 3.6, 6.52, 8, 10, 26, 85, 278 and 500 respectively in Example 6.3.

[7] W. Chen, Y. Liu, C. Wang, and S. Wise. An optimal-rate convergence analysis of a fully discrete finite difference scheme for Cahn-Hilliard-Hele-Shaw equation. *Math. Comp.*, 85:2231–2257, 2016.

[8] W. Chen, C. Wang, S. Wang, X. Wang, and S. Wise. Energy stable numerical schemes for a ternary Cahn-Hilliard system. *J. Sci. Comput.*, 84:27, 2020.

[9] W. Chen, C. Wang, X. Wang, and S. Wise. Positivity-preserving, energy stable numerical schemes for the Cahn-Hilliard equation with logarithmic potential. *J. Comput. Phys.: X*, 3:100031, 2019.

[10] L. Cherfils, A. Miranville, and S. Zelik. The Cahn-Hilliard equation with logarithmic potentials. *Milan J. Math.*, 79(2):561–596, 2011.

[11] M. I. M. Copetti and C. M. Elliott. Numerical analysis of the Cahn-Hilliard equation with a logarithmic free energy. *Numer. Math.*, 63(1):39–65, 1992.

[12] T. Curk, J. Dobnikar, and D. Frenkel. Rational design of molecularly imprinted polymers. *Soft Matter*, 12(1):35–44, 2016.
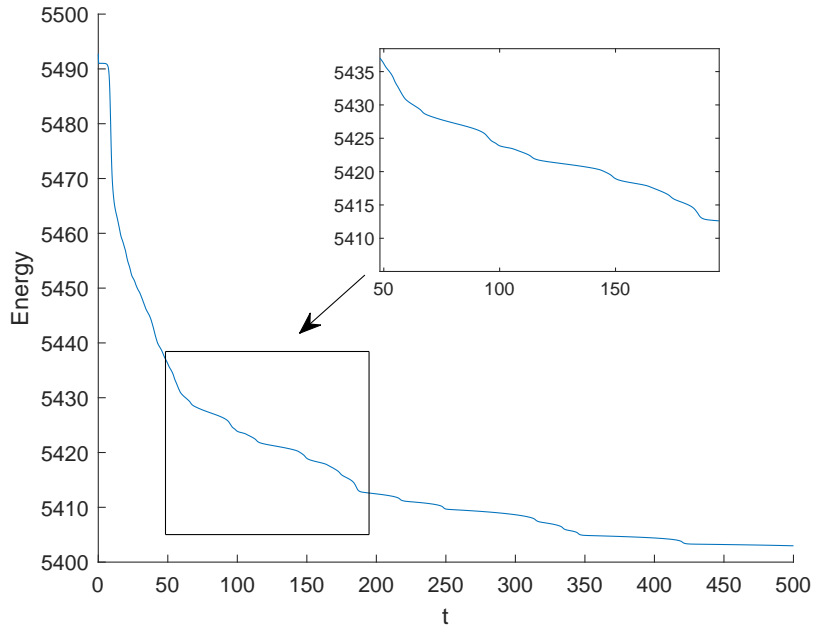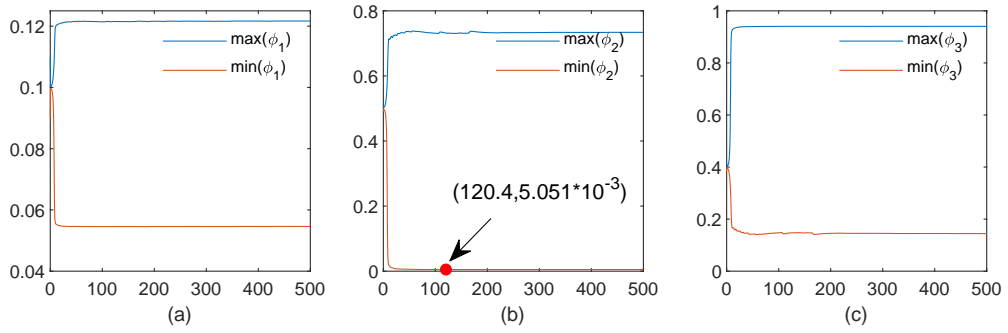
FIGURE 6.9. Energy evolution in Example 6.3.

FIGURE 6.10. Evolution of the maximum and minimum values of the phase variables ϕ_1, ϕ_2 and ϕ_3 in Example 5.2.
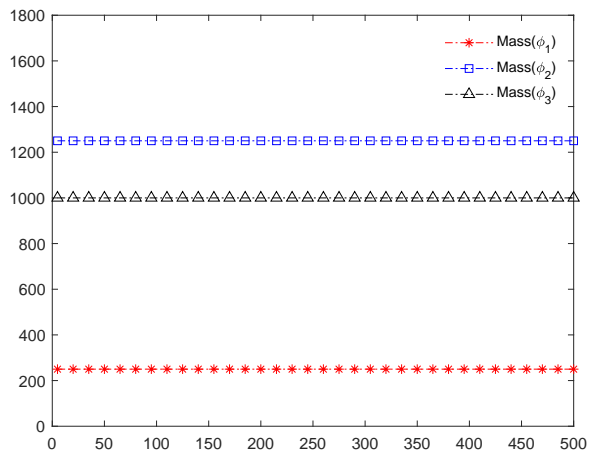

FIGURE 6.11. Mass evolution of phase variables in Example 6.3.

23

[13] A. Debussche and L. Dettori. On the Cahn-Hilliard equation with a logarithmic free energy. *Nonlinear Anal.*, 24:1491–1514, 1995.

[14] P. G. deGennes. Dynamics of fluctuations and spinodal decomposition in polymer blends. *J. Chem. Phys.*, 72:4756–4763, 1980.

[15] A. Diegel, C. Wang, X. Wang, and S. Wise. Convergence analysis and error estimates for a second order accurate finite element method for the Cahn-Hilliard-Navier-Stokes system. *Numer. Math.*, 137:495–534, 2017.

[16] A. Diegel, C. Wang, and S. Wise. Stability and convergence of a second order mixed finite element method for the Cahn-Hilliard equation. *IMA J. Numer. Anal.*, 36:1867–1897, 2016.

[17] L. Dong, C. Wang, S. Wise, and Z. Zhang. A positivity-preserving, energy stable scheme for a ternary Cahn-Hilliard system with the singular interfacial parameters. *J. Comput. Phys.*, 2021. Submitted and in review.

[18] L. Dong, C. Wang, H. Zhang, and Z. Zhang. A positivity-preserving, energy stable and convergent numerical scheme for the Cahn-Hilliard equation with a Flory-Huggins-Degennes energy. *Commun. Math. Sci.*, 17(4):921–939, 2019.

[19] L. Dong, C. Wang, H. Zhang, and Z. Zhang. A positivity-preserving second-order BDF scheme for the Cahn-Hilliard equation with variable interfacial parameters. *Commun. Comput. Phys.*, 28:967–998, 2020.

[20] J. L. Drury and D. J. Mooney. Hydrogels for tissue engineering: scaffold design variables and applications. *Biomaterials*, 24(24):4337–4351, 2003.

[21] U. Edlund, Y. Z. Ryberg, and A. Albertsson. Barrier films from renewable forestry waste. *Biomacromolecules*, 11(9):2532–2538, 2010.

[22] C. Elliott and H. Garcke. On the Cahn-Hilliard equation with degenerate mobility. *SIAM J. Math. Anal.*, 27:404, 1996.

[23] W. Feng, Z. Guan, J. Lowengrub, C. Wang, S. Wise, and Y. Chen. A uniquely solvable, energy stable numerical scheme for the functionalized Cahn-Hilliard equation and its convergence analysis. *J. Sci. Comput.*, 76(3):1938–1967, 2018.

[24] P. Flory. *Principles of Ploymer Chemistry*. Cornell University Press, New York, 1953.

[25] Y. Gong and J. Zhao. Energy-stable Runge-Kutta schemes for gradient flow models using the energy quadratization approach. *Appl. Math. Lett.*, 94:224–231, 2019.

[26] S. Gu, H. Zhang, and Z. Zhang. An energy-stable finite-difference scheme for the binary fluid-surfactant system. *J. Comput. Phys.*, 270:416–431, 2014.

[27] Z. Guan, J. Lowengrub, C. Wang, and S. Wise. Second-order convex splitting schemes for nonlocal Cahn-Hilliard and Allen-Cahn equations. *J. Comput. Phys.*, 277:48–71, 2014.

[28] Z. Guan, C. Wang, and S. Wise. A convergent convex splitting scheme for the periodic nonlocal Cahn-Hilliard equation. *Numer. Math.*, 128:377–406, 2014.

[29] J. Guo, C. Wang, S. Wise, and X. Yue. An H^2 convergence of a second-order convex-splitting, finite difference scheme for the three-dimensional Cahn-Hilliard equation. *Commun. Math. Sci.*, 14:489–515, 2016.

[30] C. He, K. Jiao, X. Zhang, M. Xiang, Z. Li, and H. Wang. Nanoparticles, microgels and bulk hydrogels with very high mechanical strength starting from micelles. *Soft Matter*, 7(6):2943–2952, 2011.

[31] T. Huang, H. Xu, K. Jiao, L. Zhu, H. R. Brown, and H. Wang. A novel hydrogel with high mechanical strength: A macromolecular microsphere composite hydrogel. *Advanced Materials*, 19(12):1622–1626, 2007.

[32] G. Ji, Y. Yang, and H. Zhang. Modeling and simulation of a ternary system for macromolecular microsphere composite hydrogels. *East Asian J. Appl. Math.*, 11(1):93–118, 2021.

[33] J. A. Johnson, N. J. Turro, J. T. Koberstein, and J. E. Mark. Some hydrogels having novel molecular structures. *Progress in Polymer Science*, 35(3):332–337, 2010.

[34] X. Li, G. Ji, and H. Zhang. Phase transitions of macromolecular microsphere composite hydrogels based on the stochastic Cahn-Hilliard equation. *J. Comput. Phys.*, 283:81–97, 2015.

[35] X. Li, Z. Qiao, and H. Zhang. An unconditionally energy stable finite difference scheme for a stochastic Cahn-Hilliard equation. *Sci. China Math.*, 59(9):1815–1834, 2016.

[36] D. Liao, H. Zhang, and Z. Zhang. Energy stable numerical method for the TDGL equation with the reticular free energy in hydrogel. *J. Comput. Math.*, 35(1):37–51, 2017.

[37] C. Liu, C. Wang, and Y. Wang. A structure-preserving, operator splitting scheme for reaction-diffusion equations with detailed balance. *J. Comput. Phys.*, 436:110253, 2021.

[38] C. Liu, C. Wang, S. Wise, X. Yue, and S. Zhou. A positivity-preserving, energy stable and convergent numerical scheme for the Poisson-Nernst-Planck system. *Math. Comp.*, 2021. Accepted and in press: arXiv:2009.08076.

[39] Y. Liu, W. Chen, C. Wang, and S. Wise. Error analysis of a mixed finite element method for a Cahn-Hilliard-Hele-Shaw system. *Numer. Math.*, 135:679–709, 2017.

[40] A. Miranville and S. Zelik. Robust exponential attractors for Cahn-Hilliard type equations with singular potentials. *Math. Methods Appl. Sci.*, 27:545–582, 2004.

[41] Y. Qian, C. Wang, and S. Zhou. A positive and energy stable numerical scheme for the Poisson-Nernst-Planck-Cahn-Hilliard equations with steric interactions. *J. Comput. Phys.*, 426:109908, 2021.

[42] J. Shen, C. Wang, X. Wang, and S. Wise. Second-order convex splitting schemes for gradient flows with Ehrlich-Schwoebel type energy: Application to thin film epitaxy. *SIAM J. Numer. Anal.*, 50:105–125, 2012.

[43] V. Thomèe. *Galerkin finite element methods for parabolic problems.* Springer, Berlin, 2006.

[44] C. Wang, X. Wang, and S. Wise. Unconditionally stable schemes for equations of thin film epitaxy. *Discrete Contin. Dyn. Syst.*, 28:405–423, 2010.

[45] C. Wang and S. Wise. An energy stable and convergent finite-difference scheme for the modified phase field crystal equation. *SIAM J. Numer. Anal.*, 49:945–969, 2011.

[46] X. Wang and H. Wang. Advances in the fabrication of hydrogels with well-defined structure and high mechanical strength. *Polymer Bulletin*, 3(107):1–6, 2008.

[47] S. Wise. Unconditionally stable finite difference, nonlinear multigrid simulation of the Cahn-Hilliard-Hele-Shaw system of equations. *J. Sci. Comput.*, 44:38–68, 2010.

[48] S. M. Wise, C. Wang, and J. Lowengrub. An energy-stable and convergent finite-difference scheme for the phase field crystal equation. *SIAM Journal on Numerical Analysis*, 47(3):2269–2288, 2009.

[49] X. Xiao, L. Chu, W. Chen, and J. Zhu. Monodispersed thermoresponsive hydrogel microspheres with a volume phase transition driven by hydrogen bonding. *Polymer*, 46(9):3199–3209, 2005.

[50] Z. Xu, X. Yang, H. Zhang, and Z. Xie. Efficient and linear schemes for anisotropic Cahn-Hilliard model using the stabilized-invariant energy quadratization (S-IEQ) approach. *Comput. Phys. Commun.*, 238:36–49, 2019.

[51] Y. Yan, W. Chen, C. Wang, and S. M. Wise. A second order energy stable BDF numerical scheme for the Cahn-Hilliard equation. *Commun. Comput. Phys.*, 23(2):572–602, 2018.

[52] X. Yang. Linear, first and second-order, unconditionally energy stable numerical schemes for the phase field model of homopolymer blends. *J. Comput. Phys.*, 327:294–316, 2016.

[53] X. Yang and J. Zhao. On linear and unconditionally energy stable algorithms for variable mobility Cahn-Hilliard type equation with logarithmic Flory-Huggins potential. *Commun. Comput. Phys.*, 25(3):703–728, 2019.

[54] X. Yang, J. Zhao, Q. Wang, and J. Shen. Numerical approximations for a three-component Cahn-Hilliard phase-field model based on the invariant energy quadratization method. *Math. Model. Meth. Appl. Sci.*, 27(11):1993–2030, 2017.

[55] D. Zhai and H. Zhang. Investigation on the application of the TDGL equation in macromolecular microsphere composite hydrogel. *Soft Matter*, 9(3):820–825, 2013.

[56] J. Zhang, C. Wang, S. Wise, and Z. Zhang. Structure-preserving, energy stable numerical schemes for a liquid thin film coarsening model. *SIAM J. Sci. Comput.*, 43(2):A1248–A1272, 2021.

School of Mathematical Sciences, Beijing Normal University, Beijing 100875, P.R. China (*Email address*, MQYUAN@MAIL.BNU.EDU.CN:)

Shanghai Key Laboratory of Mathematics for Nonlinear Sciences, School of Mathematical Sciences; Fudan University, Shanghai, China 200433 (*Email address*, WBCHEN@FUDAN.EDU.CN:)

Department of Mathematics, The University of Massachusetts, North Dartmouth, MA 02747, USA (*Email address*, CWANG1@UMASSD.EDU:)

Department of Mathematics, The University of Tennessee, Knoxville, TN 37996, USA (*Email address*, SWISE1@UTK.EDU:)

School of Mathematical Sciences, Beijing Normal University and Laboratory of Mathematics and Complex Systems, Ministry of Education, Beijing 100875, P.R. China (*Email address*, ZRZHANG@BNU.EDU.CN:)